7-24-2019

Selective Hydrogen Bonding as a Driving Force for Nanoparticle Self-assembly

Haoyun Zhang
University of Pennsalvania, haoyunz@sas.upenn.edu

Selective Hydrogen Bonding as a Driving Force for Nanoparticle Self-assembly

Abstract

Self-assembly techniques have long been used to generate novel materials with interesting optical, magnetic, electronic, and catalytic properties. This project aimed to generate the ligands capable of co-assembling catalytically active metal Pd and the suitable substrates (Fe_3O_4, CeO_2). Such a system is desirable for high catalytic activities which are attained from large metal/substrate contact surface area. The ligands are expected to tune the metal/substrate ratio through self-assembly to maximum the contact area. To achieve such system, this research focused on the synthesis of suitable hydrogen bonding ligands that have a functional group capable of binding the corresponding nanoparticle (NP) surfaces as well as selectively hydrogen bonding with one another. Multiple derivatives of such hydrogen bonding host-guest systems have been synthesized and the synthetic routes are reported. The ability to form hydrogen bonds with one another was further confirmed by NMR analysis of suitable mixtures validating the ligand design

Keywords

self-assembly, hydrogen bond, host-guest molecule, organic synthesis

Disciplines

Chemistry | Materials Chemistry | Organic Chemistry

AN ABSTRACT OF THE CAPSTONE REPORT OF

Haoyun Zhang for the degree of Master of Chemical Sciences

Title: Selective Hydrogen Bonding as a Driving Force for Nanoparticle Self-assembly

Project conducted at: Department of Chemistry
University of Pennsylvania
231 S. 34th Street, Philadelphia, PA 19104-6323
Supervisor: Christopher B. Murray
Dates of Project: May 15, 2018 – July 9, 2019

Abstract approved: Christopher B. Murray, Principle Investigator

Self-assembly techniques have long been used to generate novel materials with interesting optical, magnetic, electronic, and catalytic properties. This project aimed to generate the ligands capable of co-assembling catalytically active metal Pd and the suitable substrates (Fe_3O_4, CeO_2). Such system is desirable for high catalytic activities which is attained from large metal/substrate contact surface area. The ligands are expected to tune the metal/substrate ratio through self-assembly to maxmum the contact area. To achieve such system, this research focused on the synthesis of suitable hydrogen bonding ligands that have a functional group capable of binding the corresponding nanoparticle (NP) surfaces as well as selectively hydrogen bonding with one another. Multiple derivatives of such hydrogen bonding host-guest systems have been synthesized and the synthetic routes are reported. The ability to form hydrogen bonds with one another was further confirmed by NMR analysis of suitable mixtures validating the ligand design

Selective Hydrogen Bonding as a Driving Force for Nanoparticle Self-assembly

by

Haoyun Zhang

A CAPSTONE REPORT

submitted to the

University of Pennsylvania

in partial fulfillment of
the requirements for
the degree of

Master of Chemical Sciences

Presented on July 9, 2019
Commencement on August 9, 2019

Master of Chemical Sciences Capstone Report of Haoyun Zhang presented on July 9, 2019.

APPROVED:

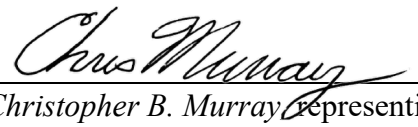

07/29/19

Prof. Christopher B. Murray, representing *Material Chemistry*

I understand that my Capstone Report will become part of the permanent collection of the University of Pennsylvania Master of Chemical Sciences Program. My signature below authorizes the release of my final report to any reader upon request.

Haoyun Zhang, Author

Acknowledgments

This work was supported by professor Christopher B. Murray's group. Special thanks to my advisor Christopher B. Murray who gave me instructions and supported for my research. Special thanks to Davit Jishkariani, who taught me characterization techniques and organic synthesis experiments. Special thanks to Ana-Rita Mayol, who instructed and guided me through every aspect of master's study program and helped me succeed. Special thanks to Murray group members Jennifer D. Lee, Katherine Elbert, Auston Keller, Natalie Gogotsi, Guillaume Gouget, and Chenjie Zeng, who helped me while completing my research. Special thanks to Keyao An for her emotional support during my master study life.

Table of Contents

List of Figures

List of Schemes

List of Appendices

Introduction

Self-assembly technology has been used broadly in nanoparticle (NP) synthesis.[1] Self-assembly is the process in which a disordered system of pre-existing components forms an organized structure or pattern as a consequence of specific, local interactions among the components themselves, without external direction.[1] While sufficiently broad to include crystallization of atomic solids, the term is generally reserved for building blocks not linked together *via* covalent bonds but ordered through weak forces.[2] Following this classification, examples of self-assembled structures include DNA, proteins, lipid vesicles, block copolymer melts, opals, and nanocrystal superlattices.[2] Self-assembly can also make use of external forces such as electric/magnetic fields or fluid flows. Apart from generating an interesting metamaterial, the self-assembly techniques have found direct applications in fields such as catalysis. For example, it can be used to engineer the surface properties of catalytically active NPs. In reactions where the cooperation between active NPs and the substrate effects on the catalyst's efficiency, the self-assembly can be used to maximize the surface to surface interaction yielding a better catalytic system.

An example of this is found in previous research done by Murray's group where the Pd@CeO_2 core-shell nanostructures are successfully fabricated by self-assembly.[3] Previous research done by Murray's group has shown the successful fabrication of Pd@CeO_2 core-shell nanostructures by self-assembly.[3] They firstly used 11-mercaptoundecanoic acid (MUA) to coat Pd NPs, then exploited $Ce(OR)_4$ alkoxide precursors to grow the ceria NPs on the outside of the Pd particles. This was followed by controlled hydrolysis where the molecular Ce(IV) alkoxides were hydrolyzed to $Ce(OH)_4$ firstly, then $Ce(OH)_4$ were converted to be catalytically relevant CeO_2, which bonded with the Pd nanoparticles to obtain dispersible Pd@CeO_2 core-shell nanostructures shown in **Figure 1**. The core-shell structure is particularly important as it increases Pd to ceria surface contact area and therefore furnishes an efficient catalyst.[3]

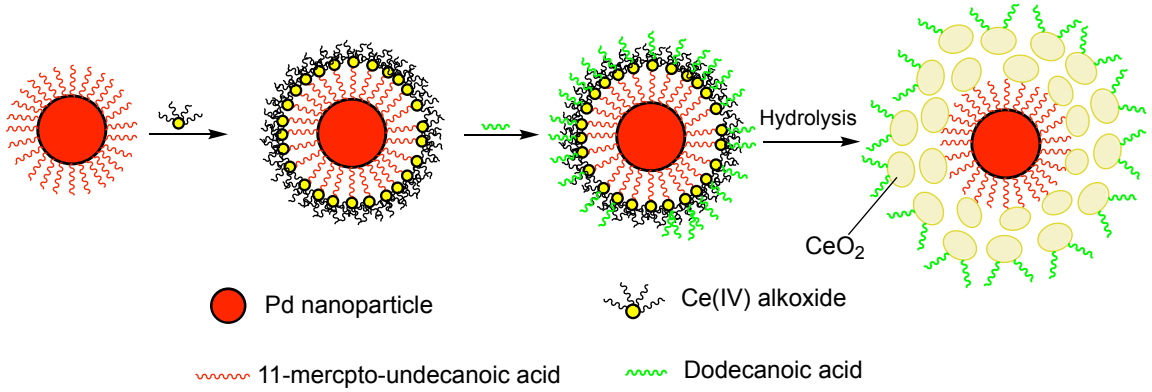

Figure 1. Schematic representation of the procedure to obtain dispersible Pd@CeO_2 core-shell nanostructures.[3]

In the field of catalysis chemistry, the above-mentioned example shows the significance of the spatial control of the NPs with respect to one another where the desired reactions often take place at the junction of two components.[3] In another example, Murray's previous research[4-6] has shown catalysis activities depends on the contact surface area between

metals. Thus, the further control of the size, shape and the position of the NPs would most certainly increase the toolbox available for researchers and perhaps allow a greater activity catalyst to be discovered.

Amongst literature reported methods to control the NPs position and spatial arrangement, the DNA guided self-assembly emerges as an extremely flexible method.[7] This approach relies on DNA recognition to be the motivation of selective hydrogen bonding between the NPs, thus providing high selectivity and orthogonality. **Figure 2** shows the selected example of preparing DNA coated magnetic NPs which uses a DNA based recognition. A magnetic probe coated with three different DNA capture strands was treated with target DNA. It was then exposed to oligonucleotide-functionalized nanoparticle probes for specific target DNA functionalized by complementary bonds. The limitation of DNA recognition experiments is that it can only be achieved in aqueous media and moderate temperatures (37 to 40 ºC). Thus, experiments of exploiting broader reaction conditions which overcome the above-mentioned limitations while maintaining the complementary hydrogen bonding is worth to be explored.

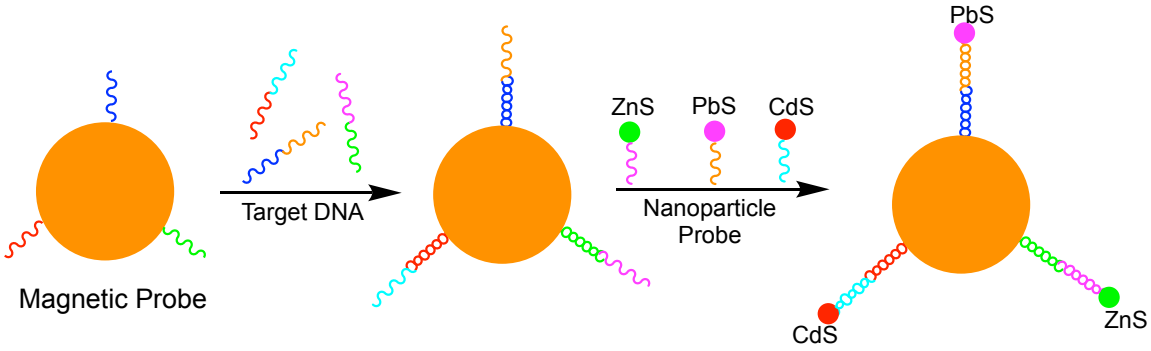

Figure 2. Magnetic microparticles (large brown spheres) coated with DNA capture strands can bind target DNA, and then oligonucleotide-functionalized nanoparticle labels (small spheres) with different electrochemical signatures can be used to code for the specific target DNA of interest.[7]

Applying host-guest molecule chemistry will allow for selectively coating the catalytically active NPs and the support materials to achieve a system where the ratio can be tuned, and the high surface contact area can be achieved (**Figure 3)**. Nanoparticles coated with complementary ligands (**Figure 3a**) can interact with the ligand pair (**Figure 3b**) selectively via hydrogen bonding (**Figure 3c)**. **Figure 3d** displays examples of selectively bonded nanostructure and **Figure 3e** shows the core structure of hydrogen bond guided self-assembly product. In terms of hydrogen bonding, the ligands are designed to have functional groups capable of binding one another selectively. The **Figure 3** shows the structures of the groups.

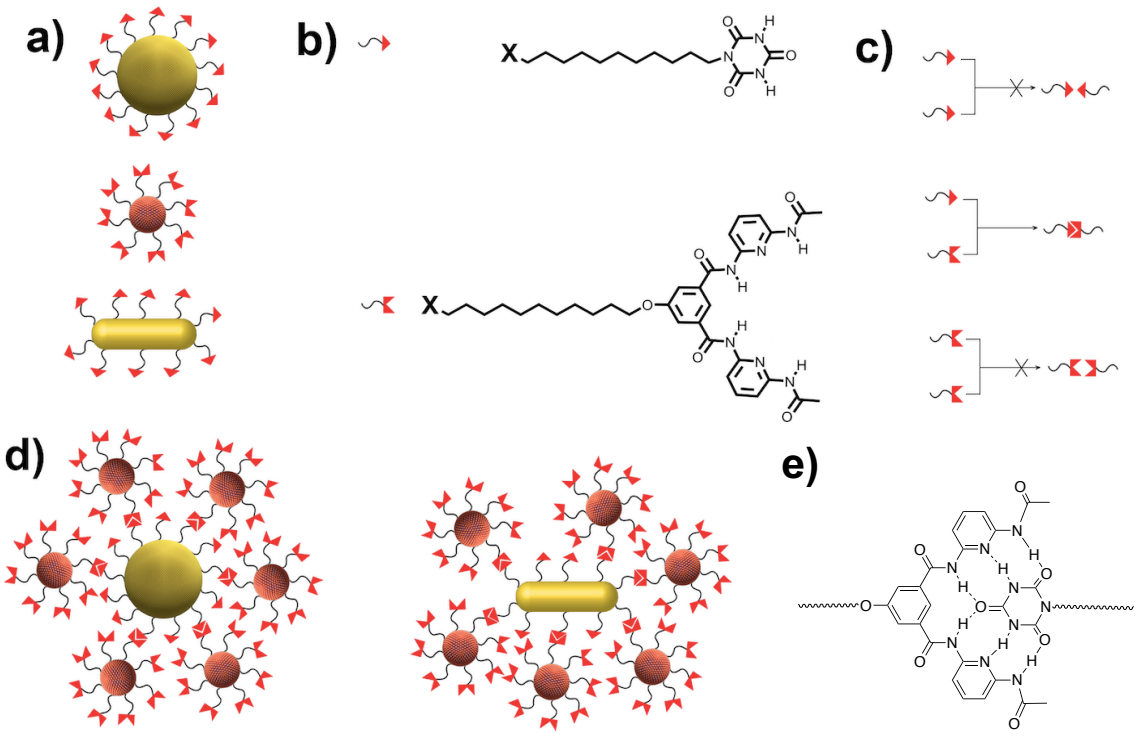

Figure 3. Schematic representation of hydrogen bonded guided self-assembly, a) building blocks coated with complementary ligands, b) ligand pair, c) hydrogen bonding complementarily, d) few examples of possible structures that can be selectively obtained and **e)** the core structure of hydrogen bond guided self-assembly product.

The goal of this work is to identify reaction conditions to synthesize host-guest molecuels that will later be applied in the preparation of NPs using self-assembly. Othe objectives of this research are to: 1) synthesize and identify optimal reaction conditions for the guest and host molecules, and 2) perform host-guest bonding studies. The approach is to identify optimal conditions in which NP ligands can be prepared in organic media while can still be assembled using the selective hydrogen bonding.

Figure 4 summarizes the synthetic approach, divided in three parts: Synthesis of precursors, Synthesis of host molecules, and host-guest molecules bonding study. Precursors **1** and **2** will be used to synthesize host molecules. The thionyl group in Precursor **1** is expected to be bind Ce and CeO_2, in future studies. Precursor **2** contains an alkyne group that is expected to undergo click chemistry with azides and subsequently bonded with Fe, Pt and Fe_3O_4. The target host molecules contain amide groups, which is expected to be the most challenging step due to steric effects, thus optimization of reaction conditions will be completed. After synthesis of host molecules, the host-guest bonding will be studied. This experiment will show the difference of interaction between host molecules and guest molecules

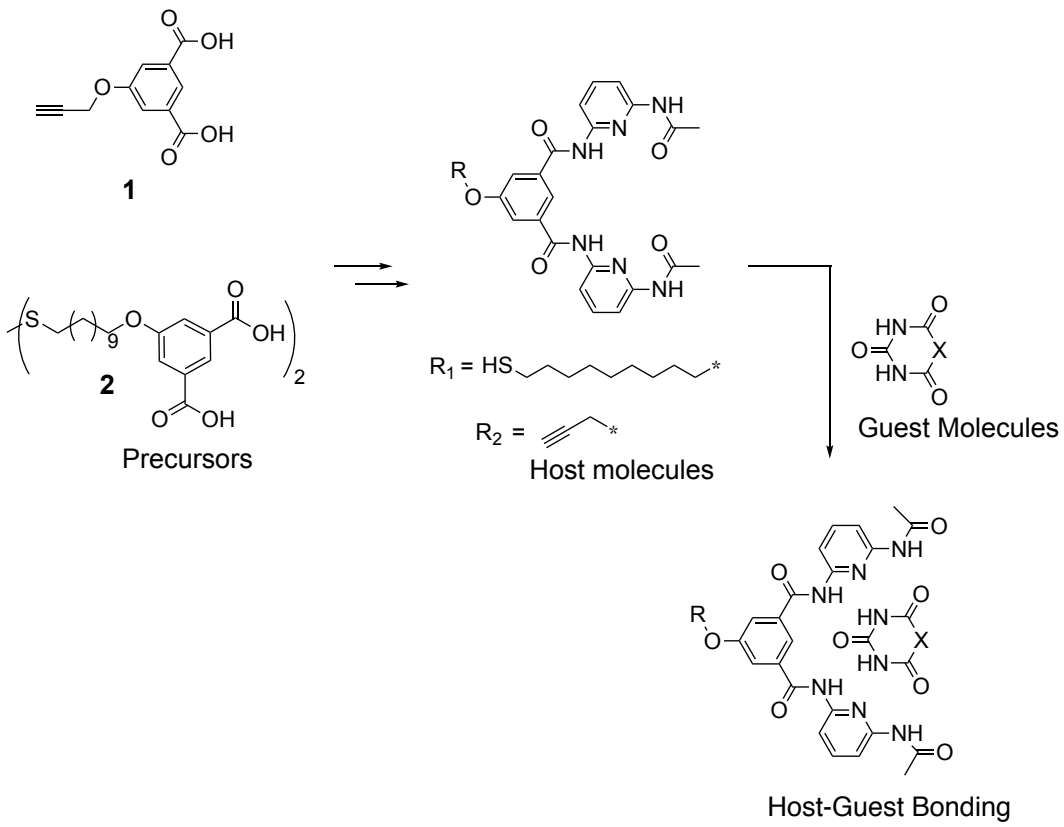

Figure 4. Synthetic approach

The target guest molecules are required to contain the specific chemical functional groups the carbonyl (C=O) and N-H bonds are required to exploit hydrogen bonding in the host-guest chemistry. Conditions of two different guest molecules will be optimized. Structures of two target guest molecules are shown in **Figure 5**. Both guest molecules **3** and **4** have a terminal alkyne which can undergo click reactions in future studies.

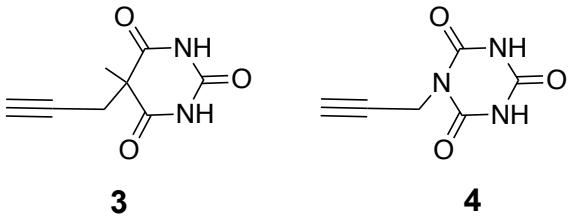

Figure 5. Structures of two different guest molecules **3** and **4**.

Materials and Methods

Materials

11-mercaptoundecanoic acid (95 %), 4-toluenesulfonyl chloride (≥ 99 %), thionyl chloride (97 %), oxalyl chloride (98 %), 2-aminopyridine (99 %), 2,4-diaminopyridine (≥ 98 %), 2-acetamido-6-aminopyridine (97 %), cyanuric acid (≥ 98 %), tosyl chloride (≥ 98 %), urea (≥ 99 %), N-(3-dimethylaminopropyl)-N′-ethylcarbodiimide hydrochloride (EDC·HCl) (97 %), 4-dimethylamino pyridine (DMAP) (≥ 99 %), 1,8-Diazabicyclo[5.4.0]undec-7-ene (DBU) (≥ 98 %), Hydroxybenzotriazole (HOBt) (97 %), 4-Pyrrolidinopyridine (4-PPY) (98 %) are purchased from Sigma-Aldrich and used without further purification. All chemicals were used as received. Potassium carbonate (reagent grade), sodium sulfate (anhydrous, reagent grade), silica gel (230-400 mesh, grade 60). Dimethyl 5-(propargyloxy) isophthalate, 5-(propynyloxy)isophthalic acid, 10-Hydroxydecyl-11'-hydroxyundecyl-1,1'-disulfide, 5-[(10-Mercaptodecyl)oxy]-1,3-benzenedicarboxylic acid **6** were synthesized according to the previously reported procedure.[15-17] Other reagents and solvents were employed as purchased. All solvents were ACS grade or higher. Dichloromethane was purchased from Fisher Scientific and was dried with activated molecular sieves (3 A, 4 to 8 mesh, purchased from Acros Organics) before use.

Techniques

NMR. ^{1}H NMR (500 MHz) and ^{13}C NMR (126 MHz) spectra were collected on a Bruker UNI500 or BIODRX500 NMR spectrometer. ^{1}H and ^{13}C chemical shifts (δ) are reported in ppm while coupling constants (J) are reported in Hertz (Hz). The multiplicity of signals in ^{1}H NMR spectra is described as "s" (singlet), "d" (doublet), "t" (triplet), "q" (quartet), "p" (pentet), "m" (mutiplet). All spectra were referenced using solvent residual signals ($CDCl_3$: ^{1}H, δ 7.27 ppm; ^{13}C, δ 77.2 ppm) and (DMSO-d_6: ^{1}H, δ 2.50 ppm; ^{13}C, δ 39.5 ppm)

Mass Spectroscopy. Electro spray ionization (ESI) was performed on Water SQD equipped with an Acuity UPLC. Matrix-assisted laser desorption/ionization time of flight (MALDI-TOF) mass spectrum was performed on a Ultraflex III (Maldi-Tof-Tof) mass spectrometer using dithranol as the matrix.

Synthetic Procedures and Details

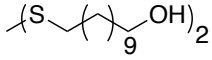

11,11'-disulfanediylbis(undecan-1-ol) 5. A solution of iodine (7.5 g, 29.4 mmol) in CH_2Cl_2 (50 mL) was added to a stirred solution of 11-mercaptoundecan-1-ol **1** (5.0 g, 24.5 mmol) in CH_2Cl_2 x mL until the solution remained purple/brown. The resulting solution stirred overnight. The reaction mixture was diluted with CH_2Cl_2 (100 mL) and washed with 1M sodium thiosulfate (2 x 100 mL). The organic layer was dried over Na_2SO_4 and concentrated under reduced pressure to afford a white solid (4.72 g, 95% yield). ^{1}H NMR ($CDCl_3$, 500 MHz) δ 3.64 (t, J = 6.6 Hz, 4H), 2.68 (t, J = 7.3Hz, 4H), 1.67 (t, 4H, J = 7.4 Hz,), 1.61 – 1.51 (m, 4H), 1.39 – 1.25 (m, 28H);^{13}C NMR ($CDCl_3$) δ 77.41, 77.16, 76.91, 63.23, 39.39, 32.96, 29.72, 29.65, 29.63, 29.57, 29.37, 28.67, 25.89; MALDI-TOF (m/z): $[M+Na]^+$ calcd. for $C_{22}H_{46}O_2S_2Na$, 429.2837; found 430.473.

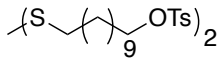

1-Undecanol-11, 11'-dithiobis-bis(4- methylbenzenesulfonate) **6**. A solution of **2** (2.04 g, 10 mmol) in methylene chloride (18 mL) in the presence of TEA (1.8 mL, 13.5 mmol) was prepared and stirred at 0 °C. Tosyl chloride (2.38 g, 13.5 mmol) was then added to the solution and the reaction mixture was stirred at ambient temperature. The resulting product was washed with water and dilute HCl. The residue from the organic layer was purified by column chromatography (Hexane: EtOAc = 8: 1) to yield the pure tosylate as a colorless oil (1.34 g, 65% yield). ^{1}H NMR ($CDCl_3$, 500 MHz): δ 7.78 (d, 4H, J = 8 Hz), 7.34 (d, 4H, J = 8 Hz), 4.01 (t, 4H, J = 7 Hz), 2.67 (t, 4H, J = 7 Hz), 1.64 (t, 4H, J = 7 Hz), 1.38-1.21 (m, 14H). ^{13}C NMR ($CDCl_3$, 500 MHz): δ 129.99, 128.07, 70.89, 39.34, 29.62, 29.60, 29.54, 29.40, 29.11, 29.01, 28.69, 25.52, 21.83; MALDI-TOF (m/z): $[M+Na]^+$ calcd. for $C_{36}H_{58}O_6S_4Na$, 739.1123; found 739.232.

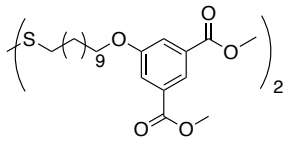

3, 3'-[dithiobis(11, 11'- dodecanediyloxy)]bis-1, 1', 5, 5'-dimethyl Benzoic ester 7. DMF solvent (50 mL) was added to a mixture of **3** (0.9 g, 2.6 mmol) and dimethyl-5-hydroxyisophthalate (1.37 g, 6.5 mmol) and stirred at ambient temperature for 20 minutes. K_2CO_3 (1.44 g, 10.4 mmol) and NaI (0.2 g) was added to above mixture which then heated to 60 °C for 6 hours. The resulting crude product was washed with 200 mL chloroform and water (4 x 100 mL) and then dried over Na_2SO_4. The mixture was removed the solvent and the residue from the organic layer was purified by column chromatography (Ratio of 4:1 Hexane: EtOAc) to yield the white powder (1.58 g, 62% yield). ^{1}H NMR ($CDCl_3$, 500 MHz): δ 8.05 (s, 2H) 7.61 (s, 4H), 4.04 (t, 4H, J = 6.5Hz), 2.65 (t, 4H, J = 5.2Hz), 2.11 (s, 12H), 1.71 (m, 4H), 1.58 (m, 4H), 1.23-1.39 (m, 28H); ^{13}C NMR ($CDCl_3$) δ 166.43, 158.80, 132.59, 122.12, 119.00, 68.07, 28.96, 28.89, 28.73, 28.56, 28.52, 27.70, 25.41, MALDI-TOF (m/z): $[M+Na]^+$ calcd. for $C_{28}H_{47}O_7S_2Na$, 661.2837; found 661.137.

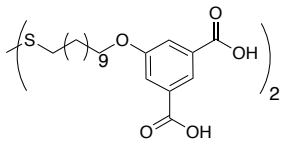

3, 3'- [dithiobis (11, 11'- dodecanediyloxy)] bis-1, 1', 5, 5'-dimethyl Benzoic acid 2. Potassium hydroxide (1.22 g, 21.77 mmol), water (10 mL) and methanol (5 mL) were added to a stirred solution of **5** in THF (10 mL). The mixture was heated to 80 °C and stirred for 4 hours. The solvents were evaporated under reduced pressure, and the resulting product was acidified with 1M HCl to afford white solid. (1.1 g, 90% yield). ^{1}H NMR (DMSO-d_6, 500 MHz): δ 8.05 (s, 2H) 7.61 (s, 4H), 4.04 (t, 4H, J = 6.5Hz), 2.65 (t, 4H, J = 5.2Hz), 1.71 (m, 4H), 1.58 (m, 4H), 1.23-1.39 (m, 28H); ^{13}C NMR (DMSO-d_6) δ 166.43, 158.80, 132.59, 122.12, 119.00, 68.07, 28.96, 28.89, 28.73, 28.56, 28.52, 27.70, 25.41, MALDI-TOF (m/z): $[M+Na]^+$ calcd. for $C_{32}H_{55}O_7S_2Na$, 605.2837; found 605.134.

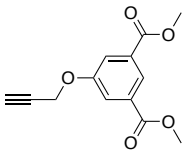

Dimethyl 5-(propargyloxy)isophthalate 8. To a round flask, dimethyl-5-hydroxyisophthalate (2 g, 9.5 mmol) and 3 equivalents of K_2CO_3 (3.9 g, 28.5 mmol) were added with 60 mL of dimethylformamide (DMF). The stirred mixture was dropwisely added 3 equivalents of propargyl bromide with a syringe. Then the mixture was heated to 85 °C overnight, and afterward removed DMF under vacuo. The reaction mixture was then suspended in NaOH (800 mg in 80 mL deionized water) and refluxed for 4 h. After cooling to room temperature, the mixture was acidified with 1 M HCl, and the white precipitate was filtered off and dried in vacuo (1.9 g, 81% yield). ^{1}H NMR (DMSO-d_6, 500 MHz): δ 8.11 (t, 1H, J = 1.5Hz) 7.72 (d, 2H, J = 1.5Hz), 4.95 (d, 2H, J = 2.5Hz), 3.63(t, 1H, J = 2.5Hz), 2.11(s, 6H); ^{13}C NMR (DMSO-d_6) δ 166.33, 157.35, 132.67, 122.92, 119.64, 78.99, 78.70, 55.99, MALDI-TOF (m/z): $[M+Na]^+$ calcd. for $C_{13}H_{13}O_5Na$, 272.2342; found 272.102.

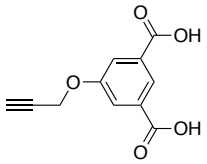

5-(Propynyloxy) isophthalic acid 1. Water (10 mL) and methanol (5 mL) and four equivalents of NaOH were added to a stirred solution of **7** (1.9 g, 7.7 mmol) in THF (10 mL), which then heated to 80 °C for 4 hours. After cooling to room temperature, the mixture was acidified with 1 M HCl to afford white solid (1.5 g, 90% yield). ^{1}H NMR (DMSO-d_6, 500 MHz): δ 8.11 (t, 1H, J = 1.5Hz) 7.72 (d, 2H, J = 1.5Hz), 4.95 (d, 2H, J = 2.5Hz), 3.63 (t, 1H, J = 2.5Hz); ^{13}C NMR (DMSO-d_6) δ 166.33, 157.35, 132.67, 122.92, 119.64, 78.99, 78.70, 55.99, MALDI-TOF (m/z): $[M+Na]^+$ calcd. for $C_{11}H_8O_5Na$, 244.1802; found 24.152.

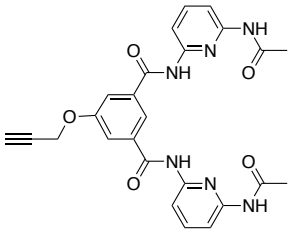

N1, N3- bis[6-[(1-methyl) amino] -2-pyridinyl] -5- (2-propyn-1-yloxy)-1, 3-benzenedicarboxamide 9. To a solution of 5-propargyloxyisophthalic acid (2.2 g, 10.0 mmol) in DMF (50 mL), 2-acetamido-6-aminopyridine (3.64 g, 24.0 mmol), (3-dimethylaminopropyl)-N′-ethyl carbodiimide hydrochloride (EDC·HCl) (5.7 g, 24.0 mmol) and Hydroxybenzotriazole (HOBt) (0.1 g, 0.7 mmol) were added and the mixture stirred at 80 °C for 2 days. After the reaction was completed, the mixture was extracted with H_2O (100 mL x 4) and CH_2Cl_2 (200 mL). The combined organic extracts were removed with a rotary evaporator and the residue was purified by column chromatography (CH_3OH/CH_2Cl_2, 1: 100 v/v as the eluent), then added 20mL chloroform and filtered to

provide **15** as a white solid (0.5 g, 10%). ^{1}H NMR (DMSO-d_6, 500 MHz): δ 10.49 (s, 2H) 10.17 (s, 2H), 8.17 (t, 1H, J = 1.5Hz), 7.84 – 7.77 (m, 8H), 5.00 (d, 2H, J = 2.5Hz), 3.66 (t, 1H, J = 2.5Hz), 2.12 (s, 6H), ^{13}C NMR (DMSO-d_6) δ 165.32, 157.82, 152.44, 148.50, 138.83, 135.93, 120.55, 118.26, 114.90, 56.53, 46.17, MALDI-TOF (m/z): $[M+Na]^+$ calcd. for $C_{25}H_{23}N_6O_5$, 487.1802; found 287.252.

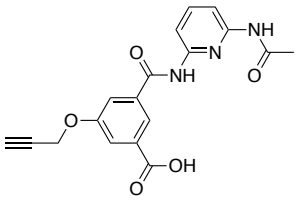

N-6-[(1-methyl)amino]-2-pyridinyl]-3-carboxyl-5-(2-propyn-1-yloxy)-benzenemonocarboxamide 10. 2-acetamido-6-aminopyridine (3.64 g, 24.0 mmol), (3-dimethylaminopropyl)-N′-ethylcarbodiimide hydrochloride (EDC·HCl) (5.7 g, 24.0 mmol) and 4-dimethylaminopyridine (DMAP) (0.1 g, 0.7 mmol) were added to a solution of 5-propargyloxyisophthalic acid (2.2 g, 10.0 mmol) in CH_2Cl_2 (50 mL). Then the mixture was stirred at room temperature for 3 days. Upon reaction completion, the mixture was extracted with H_2O (100 mL x 4) and CH_2Cl_2 (200 mL). The combined organic extracts were removed with a rotary evaporator, and the residue was purified by column chromatography (CH_3OH/CH_2Cl_2, 1: 100 v/v as the eluent) to provide **10** as a white solid (0.8 g, 23%). ^{1}H NMR (DMSO-d_6, 500 MHz): δ 10.58 (s, 1H) 10.28 (s, 1H), 8.12 (t, 1H, J = 1.5Hz), 7.81 – 7.69 (m, 5H), 4.96 (d, 2H, J = 2.5Hz), 3.61 (t, 1H, J = 2.5Hz), 2.10 (s, 3H), ^{13}C NMR (DMSO-d_6) δ 165.32, 157.82, 152.44, 148.50, 138.83, 135.93, 120.55, 118.26, 114.90, 56.53, 46.17, MALDI-TOF (m/z): $[M+Na]^+$ calcd. for $C_{18}H_{15}N_3O_5Na$, 377.1231; found 377.321.

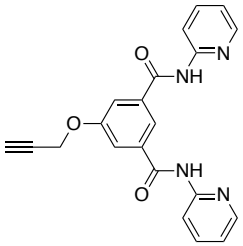

N1, N3-bis(2-pyridinyl)-5-(2-propyn-1-yloxy)-1, 3-benzenedicarboxamide 11. 2-aminopyridine (3.64 g, 24.0 mmol), EDC·HCl (5.70 g, 24.0 mmol) and HOBt (0.10 g, 0.7 mmol) were added to a solution of 5-propargyloxyisophthalic acid (2.20 g, 10.0 mmol) in CH_2Cl_2 (50 mL). Then the mixture was stirred at 80 °C for 2 days. After the reaction was completed, the mixture was extracted with H_2O (100 mL x 4) and CH_2Cl_2 (100 mL). The combined organic extracts were removed with a rotary evaporator and the residue was purified by column chromatography (CH_3OH: CH_2Cl_2 = 1: 100 v/v as the eluent to provide **11** as a white solid (0.8 g, 40.3%). ^{1}H NMR (DMSO-d_6, 500 MHz): δ 10.80(s, 2H), 8.40-8.43(m, 2H), 8.30(t, 1H), 8.25 (d, 2H, J = 2.5Hz), 7.86-7.90 (m, 2H), 7.78 (d, 2H, J = 1.5Hz), 5.00 (d, 2H, J = 2.5Hz), 3.66 (t, 1H, J = 2.5Hz); ^{13}C NMR (DMSO-d_6) δ 165.32, 157.82, 152.44, 148.50, 138.83, 135.93, 120.55, 118.26, 114.90, 56.53, 46.17. MALDI-TOF (m/z): $[M+Na]^+$ calcd. for $C_{21}H_{17}N_4O_3Na$, 396.3822 found 396.112.

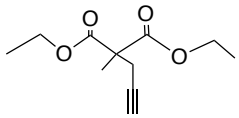

Diethyl propargylmethylmalonate 12. Diethy methylmalonate (1.50 g, 0.080 mol) dissolved in DMF (5 mL) was added dropwisely to the slurry of NaOEt (0.68 g, 0.100 mol) in DMF (83 mL) at 0 ºC. After stirring the reaction mixture for 20 minutes, propargyl chloride (0.718 g, 0.096 mol) in DMF (5 mL) was added dropwise to the reaction mixture in iced bath. After this reaction mixture was stirred at room temperature for 6 hours, it was treated with saturated ammonium chloride solution, and extracted with ethyl acetate. Combined organic layer was washed with brine, and dried over anhydrous $MgSO_4$. The solvents were evaporated, and the resulting brown oil was purified by flash column chromatograph (ratio of ethyl acetate: n-hexane 2:5) to afford **12** as slight brown oil. (1.52 g, 80 % yield). ^{1}H NMR (500 MHz, DMSO-d_6) δ 4.19 (q, J = 7.1Hz, 4H), 2.81 (d, J = 2.7Hz, 2H), 2.09 (q, J = 7.6Hz, 2H), 1.99 (t, J = 2.7Hz, 1H), 1.25 (t, J = 7.1Hz, 6H), 0.87 (t, J = 7.6Hz, 3H). ^{13}C NMR (DMSO-d_6) δ 170.5, 74.2, 61.7, 52.9, 25.6, 19.7, 14.2. MALDI-TOF (m/z): $[M+Na]^+$ calcd. for $C_{11}H_{16}O_4Na$, 235.1729 found 235.23.

Results and Discussion

Synthesis of Precursors

The synthesis steps of precursor **1** is shown in **Scheme 1**. The first step is to functionalize the phenol group by propyl bromide. Precursor **1** can be hydrolyzed from the diester **5** with a yield of 90%. Synthesis of the precursor **2** is shown in **Scheme 2**. The starting material 11-mercaptoundecanoic acid was dimerized by using iodine to protect the thiol group. Then the dimer was reacted with 4-Toluenesulfonyl chloride (TsCl) to obtain **7** which now contains a tosyl leaving group. Replacement of the tosyl group with phenolic oxygen of dimethyl 5-hydroxyisophthalate leaded to the isophthalate precursor **2** in 90% yield.

Scheme 1. Synthetic routes of isophthalate precursor **1**

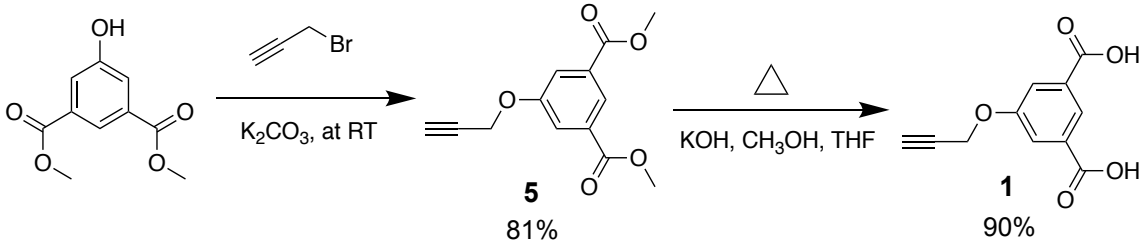

Scheme 2. Synthetic routes of isophthalate precursor **2**

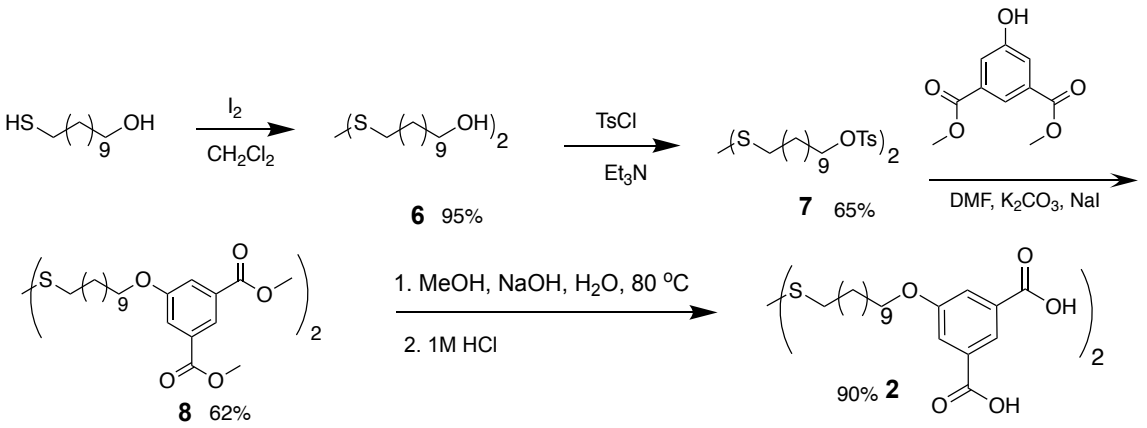

Synthesis of Host Molecules

*Optimization of Reaction Conditions for Host Molecule **9***

Two pathways were used to synthesize host molecule **9** as shown in **Scheme 3.** Precursor **1** was used as the starting point using reaction conditions based on previous work.[6,7] Precursor **1** was treated with sulfonyl chloride or oxalyl chloride to generate 5-(Propynyloxy) isophthalic benzoyl chloride which was then reacted with 2-aminopyridine. Only trace amounts of the diamide compounds **9** obtained. The intermediate 5-(Propynyloxy) isophthalic benzoyl chloride is not stable and could not to be isolated. This might interfere with the overall yield of the reaction.

Scheme 3. Two pathways of synthesizing host molecule **9** via benzoyl chloride intermediate.[6,7]

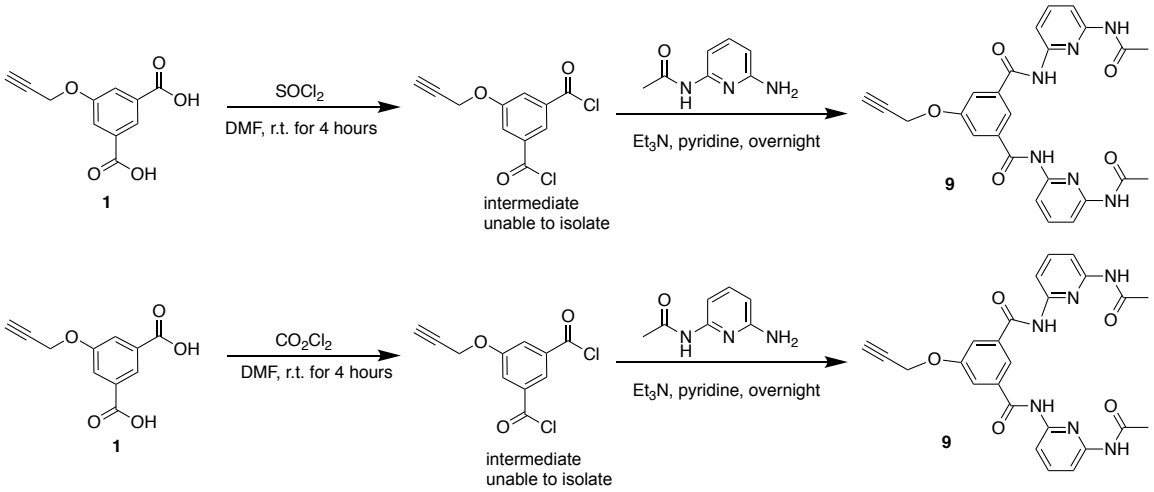

Due to that 2-acetamido-6-aminopyridine is expensive and has low reactivity, different pathways were explored to identify the optimized reaction conditions by using more readily available 2-aminopyridine. The host molecule **11** was synthesized by using EDCl as coupling reagent and DMAP as catalyst (**Scheme 4)**. A 40% yield of diamide compound **11** was obtained. After this exploration, the same reaction conditions were exploited on synthesis of host molecule **9**, which instead used 2-acetamido-6-aminopyridine was used as the amino source (**Scheme 5**). However, only a yield of 23% was obtained for the monosubstituted product **10** and trace amounts of the disubstituted product **9** was formed. This might be due to: 1) the electrowithdrawing group present in 2-acetamido-6-aminopyridine resulting in lower reactivity; 2) the EDCl coupling reagent might not be as effective to produce the disubstituted product **9**. Therefore, the stronger coupling agent HOBt was exploited on this reaction and 10% yield of **9** was obtained while trace monosubstituted product **10** was formed (**Scheme 6**). Although the yield of **9** was only 10%, the successful synthesis of host molecule **9** was achieved. This proved that the stronger coupling reagent HOBt is the necessary to obtain the desired diamide product.

Scheme 4. Catalytic method of synthesizing host molecule **11**

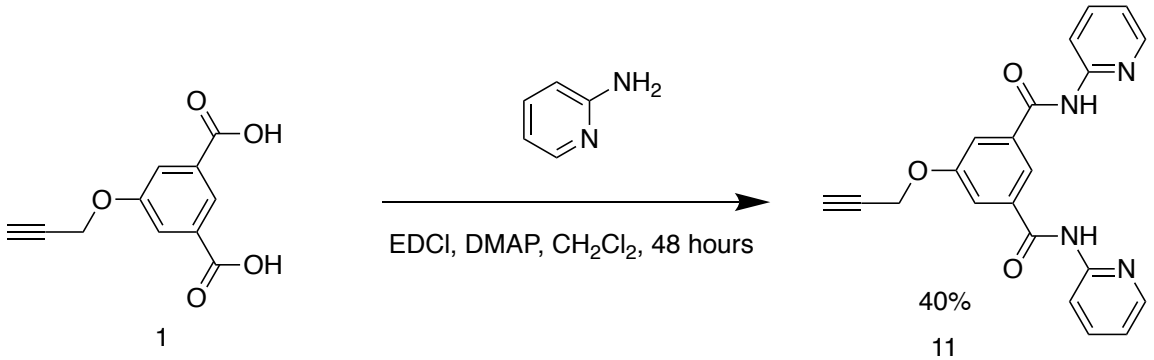

Scheme 5. Catalytic route to synthesize host molecule **9** by using DMAP as catalyst.

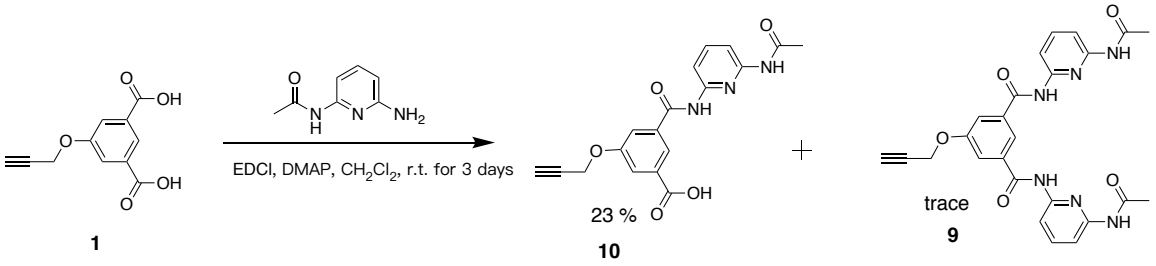

Scheme 6. Catalytic route to synthesize host molecule **9** by using HOBt as coupling reagent.

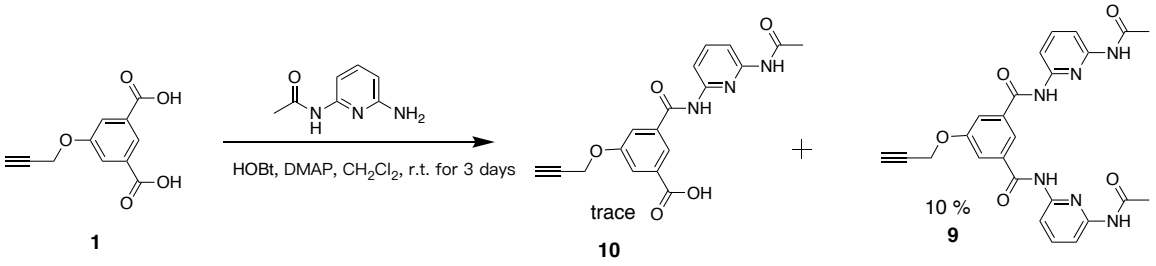

Optimization of Reaction Conditions for Host Molecule 13

For the host molecule **13**, the optimization of reaction conditions was explored by two different methods. The first method is shown in **Scheme 7**. Precursor **2** was reacted with sulfonyl chloride or oxalyl chloride to generate 5-(Propynyloxy) isophthalic benzoyl chloride intermediate which was then reacted with 2-acetamido-6-aminopyridine. Only trace amounts of diamide product **13** was formed. Since the intermediate is too active and could not be isolated, it might restrict the overall yield of the reaction.

Scheme 7. Two pathways of synthesizing host molecule **13** via benzoyl dichloride intermediates

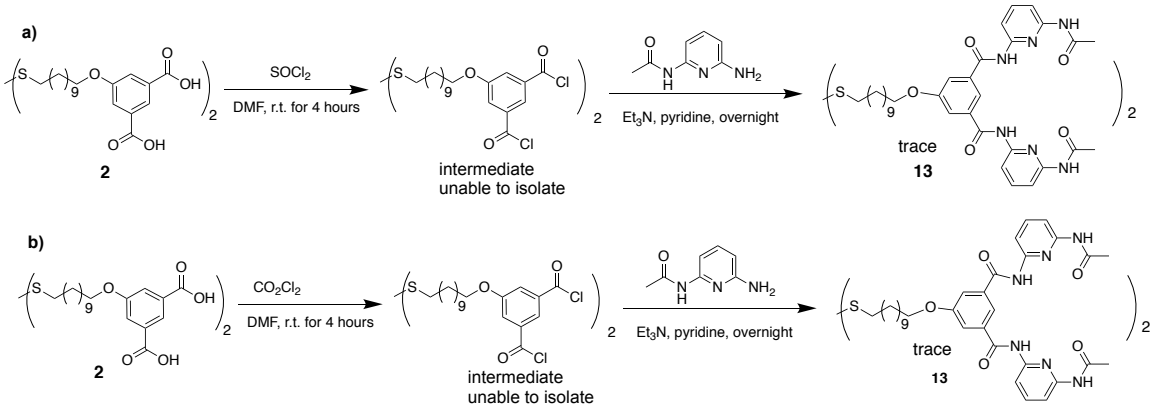

The second method, shown in **Scheme 8,** explored different combinations of catalysts and coupling reagents to optimize the reaction condition. **Scheme 8a** used EDCl as coupling agent and DMAP as catalyst while **Scheme 8b** used HOBt as the coupling reagent. The catalytic activity of 4-PPY is thousands times better than DMAP.[15] Therefore **Scheme 8c** used 4-(1-Pyrrolidinyl) pyridine (4-PPY) as the catalyst and EDCl as coupling reagent. There were trace amount of diamide products formed by three pathways. This result

showed that the low yield might not be because of catalysts but due to the steric effect of Precursor **2** and the low reactivity of coupling reagents.

Scheme 8. Catalytic method to synthesize guest molecule **13**

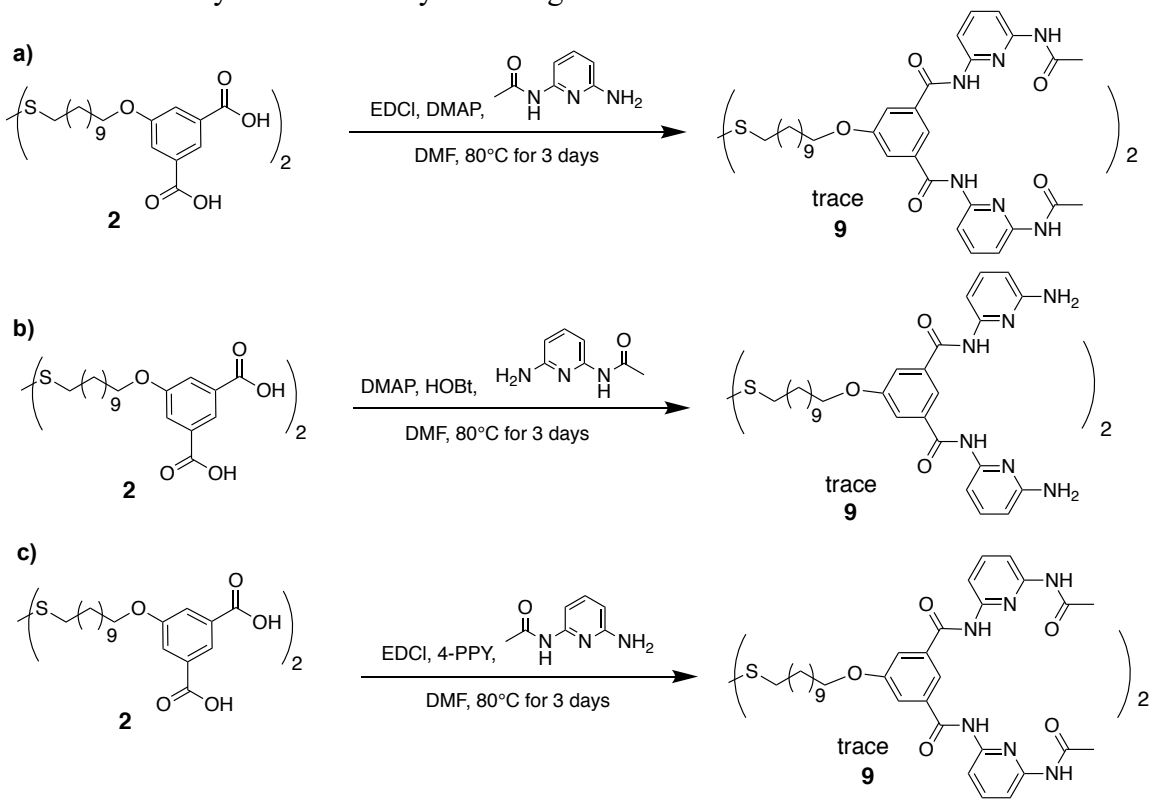

Synthesis of Guest Molecules

An approach to synthesize **3** is shown in **Scheme 9**.[8] The first step was accomplished by diethyl methylmalonate and propargyl bromide to afford 80% yield of **12**.Compound **12** was then treated with urea in order to obtain **3** (**Scheme 9**). Only trace amounts of **3** was isolated. Presumably this could be because: 1) the large polarity of guest molecule **3** hinderrs isolation via column chromatography; 2) the close polarity between side product and **3** makes it difficult for **3** to be purified by recrystallization.

Other synthetic route was utilized to afford guest molecule **4**. The cyanuric acid was reacted with propargyl bromide directly and three substituted products were obtained (**Scheme 10**). However, there was trace anmount of **4** obtained after purification. From mass spectrum, the **15** was the main product and the **4** was the minor product. Since these three substituted products have very strong and similar polarities, they are unable to be crystalized by column chromatography and difficult to be isolated by recrystallization.

Scheme 9. Synthetic routes of guest molecule **3**.[8]

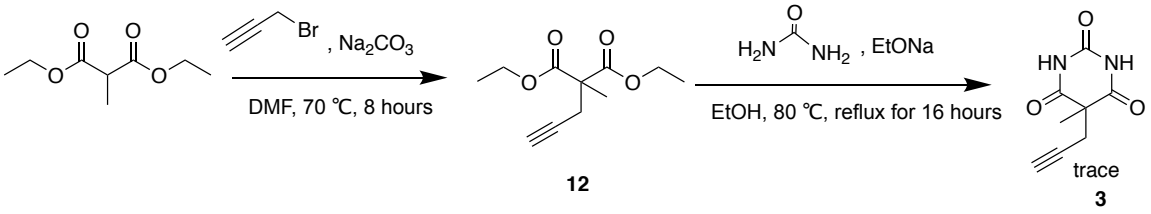

Scheme 10. Synthetic route of guest molecule **4**.

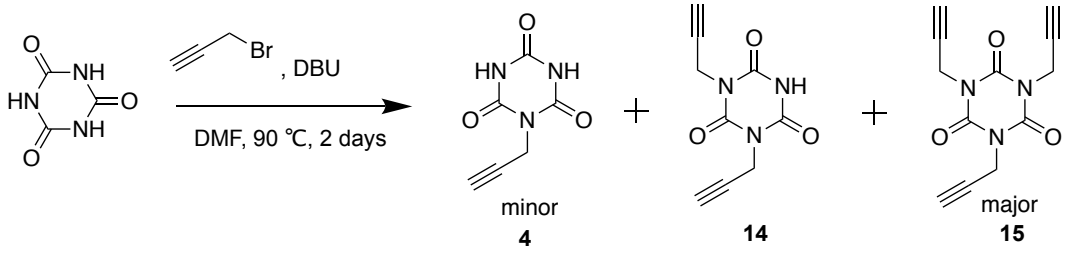

Host-Guest Bonding Studies

The guest molecules **3** and **4** were not obtained in significant amount. The interaction between host and guest molecules could to be studied using analogous molecules. Cyanuric acid has three amide groups which are similar to guest molecules **3** and **4**. The interaction of cyanuric acid and host molecules is also similar to the guest-host molecules interactions. Thus, cyanuric acid is expected to behave as target guest molecules **3** and **4**. To validate the original design of hydrogen bonding template, interactions between molecules **9, 10, 11** and cyanuric acid was tested. This was achieved by mixing equimolar amounts of suitable pair in DMSO-d_6, and the resulting spectrum was overlaid with the clean spectra of each molecule to observe the chemical shift of individual protons. The chemical shift of N-H bond of cyanuric acid can be used to probe the interaction between these host-guest complexes (**Figure 6**). **Figure 6** shows the change in chemical shift towards lower energy in all cases, denoted by dash lines. **Figure 6a** shows the partial spectrum of disubstituted host molecule **9** bonded with cyanuric acid and the partial spectrum of disubstituted molecule **11** and cyanuric acid is shown in **Figure 6b**. **Figure 6c** show the partial NMR spectrum of monosubstituted guest molecule **10** bonded with cyanuric acid and **Figrue 6d** show the cyanuric acid. The change in chemical shift is highest when complexed with disubstituted products **8** and **9** (0.14 ppm for **8** and **9** *vs* 0.03 ppm for **10**). This result proved that **8** and **9** have stronger interaction with cyanuric acid, and the most important observation here is that this data strongly suggests that the interaction between host and guest molecules designed in this study can form hydrogen bonds with one another. Therefore, the strong interaction between guest molecules and host molecule by complementary hydrogen bonds verifies the achievability of self-assembly techniques.

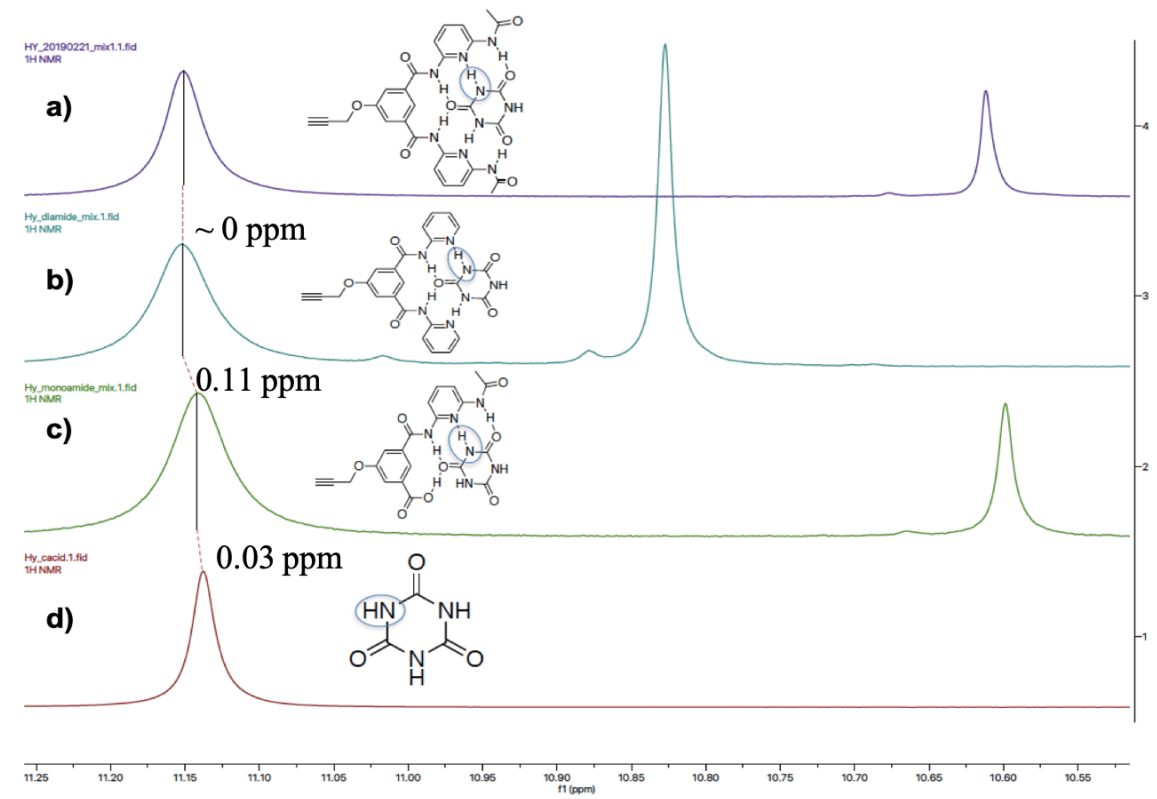

Figure 6. Partial ^{1}H NMR spectra (500 Hz, DMSO-d_6, 293 K) of a) disubstituted guest molecule **9** bonding with cyanuric acid; b) disubstituted amide molecule **11** bonding with cyanuric acid; c) monosubstituted amide **10** bonding with cyanuric acid; d) cyanuric acid.

Conclusion

In conclusion, the optimization of conditions for the synthesis of host molecules **9, 10** and **11** have been identified. The optimized conditions provide reasonably high yield from commercially available starting material **4** in three steps. Compared with thionyl chloride method, the catalytic method made it possible to control the ratio of monosubstituted and disubstituted products. When using DMAP as catalysts, only monosubstituted product can be afforded, which is hardly used in further research. After using HOBt, diamide groups were successfully formed and the host molecules were synthesized. Further work is needed to elucidate the optimal conditions to increase the yield of reactions towards the preparation of functionalized guest molecule.

Future Work

Since the synthesis steps of guest molecules **9** have been exploited successfully, future work can be accomplished by exploiting the synthesis steps of the other host molecules such as **17**. Due to the poor reactivity of 2-acetamido-6-aminopyridine, the reaction could be achieved by reacting with more active starting materials followed by treatment with pivaloyl chloride to form the desered amino groups (**Scheme 11**).

Scheme 11. possible synthesis routes of guest molecules **17**.

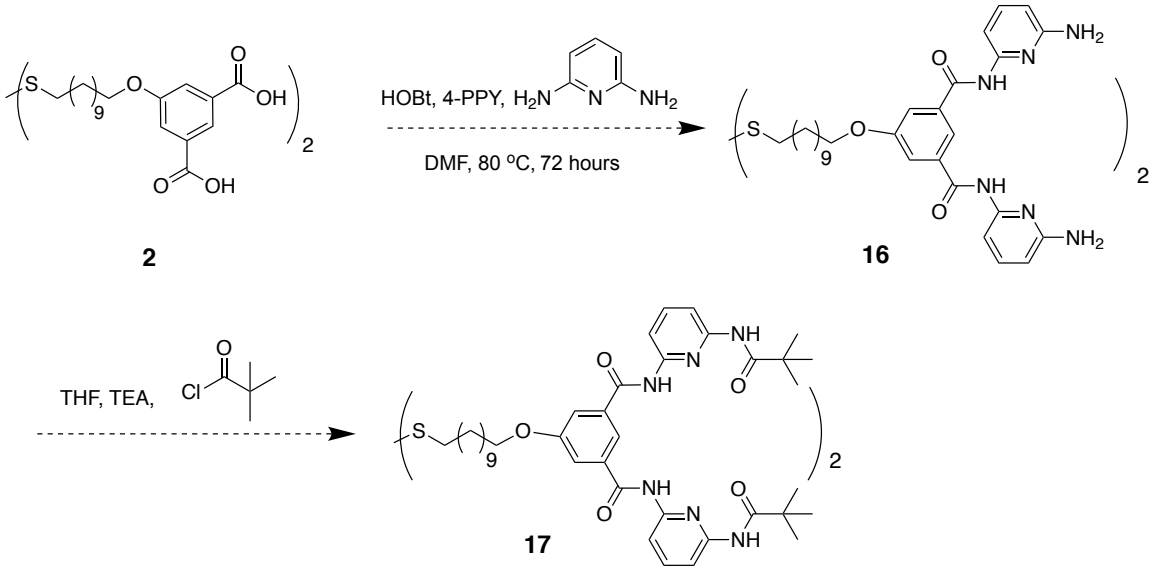

This work can be applied to obtain NPs with unique catalytic activity. The functional groups (alkyne and thiol groups) in the host molecules and guest molecules can bind with metals such as Pd, Pt, Au, Fe_2O_3, CeO_2, and Al_2O_3. Future work can be accomplished by maximizing the surface-surface interaction, leading to the large improvement in its catalytic activity such as CO oxidation catalysis, the water-gas shift catalysis, and catalysis of methanol steam reforming reaction.

References

1. Min, Y.; Akbulut, M.; Kristiansen, K.; Golan, Y.; Israelachvili, J. The Role of Interparticle and External Forces in Nanoparticle Assembly. *Nat. Mater*. **2008**, 7 (7), 527−538.
2. Pinheiro, A. V.; Han, D.; Shih, W. M.; Yan, H. Challenges and Opportunities for Structural DNA Nanotechnology. *Nat. Nanotechnol.* **2011**, 6 (12), 763−772.
3. Dill, K. A.; MacCallum, J. L. The Protein-Folding Problem, 50 Years On. *Science* **2012**, 338 (6110), 1042−1046.
4. Chen, I. A.; Walde, P. From Self-Assembled Vesicles to Protocells. *Cold Spring Harbor Perspect. Biol*. **2010**, 2 (7), a002170.
5. Bates, F. S.; Hillmyer, M. A.; Lodge, T. P.; Bates, C. M.; Delaney, K. T.; Fredrickson, G. H. Multiblock Polymers: Panacea or Pandora's Box? *Science* **2012**, 336 (6080), 434−440.
6. Kim, S.-H.; Lee, S. Y.; Yang, S.-M.; Yi, G.-R. Self-Assembled Colloidal Structures for Photonics. *NPG Asia Mater.* **2011**, 3 (1), 25−33.
7. Vogel, N.; Retsch, M.; Fustin, C.-A.; del Campo, A.; Jonas, U.Advances in Colloidal Assembly: The Design of Structure and Hierarchy in Two and Three Dimensions. *Chem. Rev*. **2015**, 115 (13),6265−6311.
8. Sun, S.; Murray, C. B.; Weller, D.; Folks, L.; Moser, A.Monodisperse FePt Nanoparticles and Ferromagnetic FePt Nanocrystal Superlattices. *Science* **2000**, 287 (5460), 1989−1992.
9. Shevchenko, E. V.; Talapin, D. V. Self-Assembly of Semiconductor Nanocrystals into Ordered Superstructures. In Semiconductor Nanocrystal Quantum Dots; Springer: *Vienna*, **2008**; pp119−169.
10. Murray, C. B.; Kagan, C. R.; Bawendi, M. G. Synthesis and Characterization of Monodisperse Nanocrystals and Close-Packed Nanocrystal Assemblies. *Annu. Rev. Mater. Sci.* **2000**, 30 (1), 545−610.
11. Pileni, M. P. Nanocrystal Self-Assemblies: Fabrication and Collective Properties. *J. Phys. Chem. B* **2001**, 105 (17), 3358−3371.
12. Rogach, A. L.; Talapin, D. V.; Shevchenko, E. V.; Kornowski, A.; Haase, M.; Weller, H. Organization of Matter on Different Size Scales: Monodisperse Nanocrystals and Their Superstructures. *Adv. Funct. Mater*. **2002**, 12 (10), 653−664.
13. Liz-Marzán, L. M.; Mulvaney, P. The Assembly of Coated Nanocrystals. *J. Phys. Chem. B* **2003**, 107 (30), 7312−7326.
14. Daniel, M.-C.; Astruc, D. Gold Nanoparticles: Assembly, Supramolecular Chemistry, Quantum-Size-Related Properties, and Applications toward Biology, Catalysis, and Nanotechnology. *Chem. Rev.* **2004**, 104 (1), 293−346.
15. Bishop, K. J. M.; Wilmer, C. E.; Soh, S.; Grzybowski, B. A. Nanoscale Forces and Their Uses in Self-Assembly. *Small* **2009**, 5 (14), 1600−1630.
16. Cargnello, M.; Doan-Nguyen, V. V. T.; Gordon, T. R.; Diaz, R. E.; Stach, E. A.; Gorte, R. J.; Fornasiero, P.; Murray, C. B. Control of Metal Nanocrystal Size Reveals Metal-Support Interface Role for Ceria Catalysts. *Science* **2013**, *341*, 771.
17. Cargnello, M.; Wieder, N. L.; Montini, T.; Gorte, R. J.; Fornasiero, P. Synthesis of Dispersible Pd@CeO2 Core−Shell Nanostructures by Self-Assembly. *J. Am. Chem. Soc.* **2010**, *132*(4), 1402.

18. Mirkin, C. A.; Letsinger, R. L.; Mucic, R. C.; Storhoff, J. J. A DNA-based method for rationally assembling nanoparticles into macroscopic materials. *Nature* **1996**, *382*, 607.
19. Jishkariani, D.; Diroll, B. T.; Cargnello, M.; Klein, D. R.; Hough, L. A.; Murray, C. B.; Donnio, B. Dendron-Mediated Engineering of Interparticle Separation and Self-Assembly in Dendronized Gold Nanoparticles Superlattices. *J. Am. Chem. Soc.* **2015**, *137*, 10728.
20. Diroll, B. T.; Weigandt, K. M.; Jishkariani, D.; Cargnello, M.; Murphy, R. J.; Hough, L. A.; Murray, C. B.; Donnio, B. Quantifying "Softness" of Organic Coatings on Gold Nanoparticles Using Correlated Small-Angle X-ray and Neutron Scattering. *Nano Letters* **2015**, *15*, 8008.
21. Hiramatsu, H.; Osterloh, F. E. A Simple Large-Scale Synthesis of Nearly Monodisperse Gold and Silver Nanoparticles with Adjustable Sizes and with Exchangeable Surfactants. *Chem. Mat.* **2004**, *16*, 2509.
22. Schmidbaur, H.; Schier, A. Coordination Chemistry at Carbon: The Patchwork Family Comprising $(Ph_3P)_2C$, $(Ph_3P)C(C_2H_4)$, and $(C_2H_4)_2C$. *Angew. Chem. Int. Ed.* **2012**, *52*, 176.
23. Chen, S.; Kimura, K. Synthesis and Characterization of Carboxylate-Modified Gold Nanoparticle Powders Dispersible in Water. *Langmuir* **1999**, *15*, 1075.
24. Laaksonen, T.; Ahonen, P.; Johans, C.; Kontturi, K. Stability and electrostatics of mercaptoundecanoic acid-capped gold nanoparticles with varying counterion size. *ChemPhysChem* **2006**, *7*, 2143.
25. Yee, C. K.; Jordan, R.; Ulman, A.; White, H.; King, A.; Rafailovich, M.; Sokolov, J. Novel One-Phase Synthesis of Thiol-Functionalized Gold, Palladium, and Iridium Nanoparticles Using Superhydride. *Langmuir* **1999**, *15*, 3486.
26. Talapin, D. V.; Shevchenko, E. V.; Bodnarchuk, M. I.; Ye, X.; Chen, J.; Murray, C. B. Quasicrystalline order in self-assembled binary nanoparticle superlattices. *Nature* **2009**, *461*, 964.
27. Avouris, P.; Freitag, M.; Perebeinos, V. Carbon-nanotube photonics and optoelectronics. *Nat. Photon.* **2008**, *2*, 341.
28. Natarajan, S.; Mandal, S. Open-framework structures of transition-metal compounds. *Angew. Chem., Int. Ed.* **2008**, *47*, 4798.
29. Daniel, M. C.; Astruc, D. Gold Nanoparticles: Assembly, Supramolecular Chemistry, Quantum-Size-Related Properties, and Applications toward Biology, Catalysis, and Nanotechnology. *Chem. Rev*. **2004**, *104*, 293.
30. Ahmadi, T. S.; Wang, Z. L.; Green, T. C.; Henglein, A.; El-Sayed, M. A. Shape-Controlled Synthesis of Colloidal Platinum Nanoparticles. *Science* **1996**, *272*, 1924.
31. Thaner, R. V.; Kim, Y.; Li, T. I. N. G.; Macfarlane, R. J.; Nguyen, S. T.; Cruz, M. O. D. L.; Mirkin, C. A. Entropy-Driven Crystallization Behavior in DNA-Mediated Nanoparticle Assembly. *Nano Letters* **2015**, *15*, 5545.

Appendices

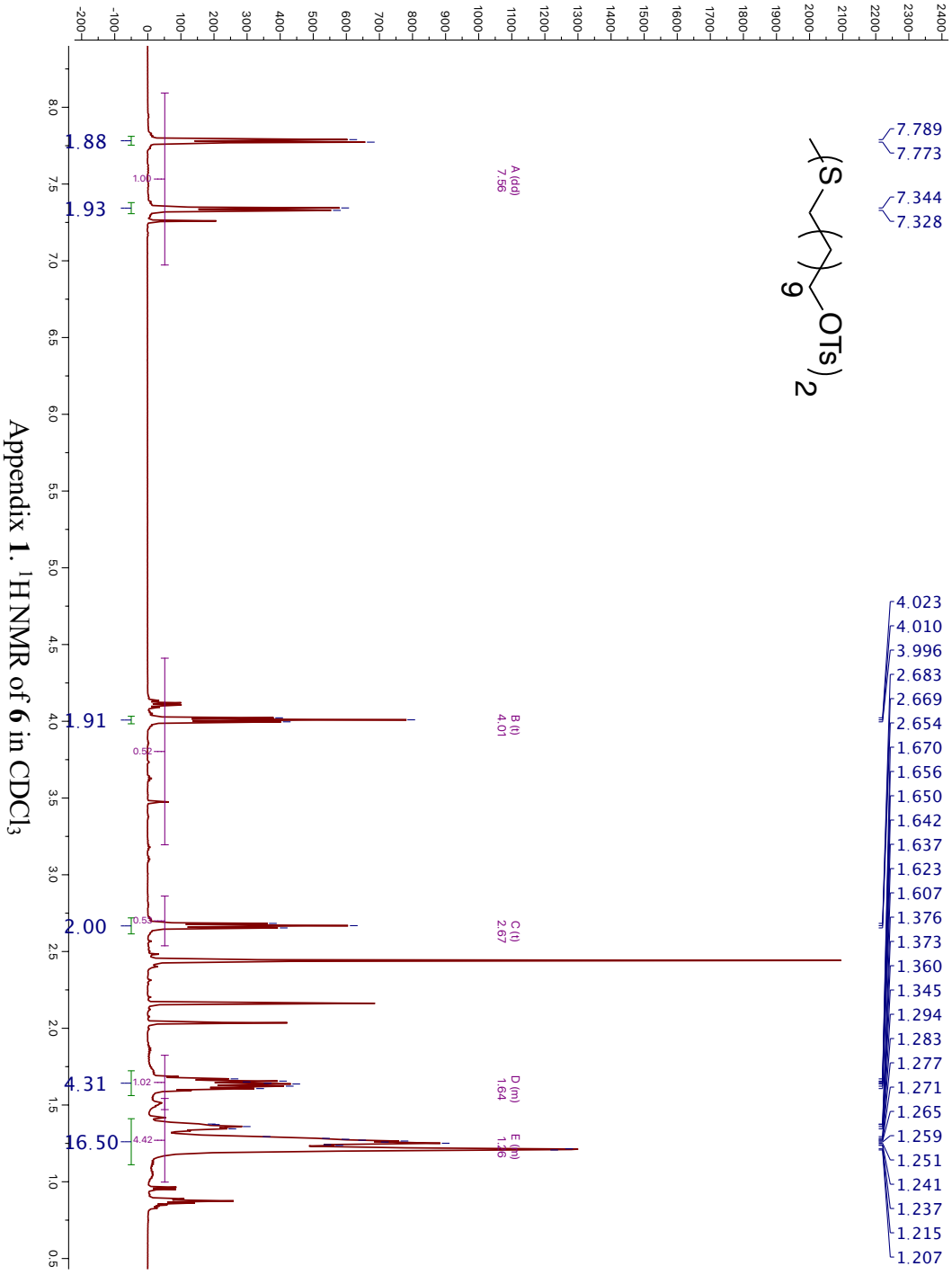

Appendix **1**. ^{1}H NMR of **6** in $CDCl_3$

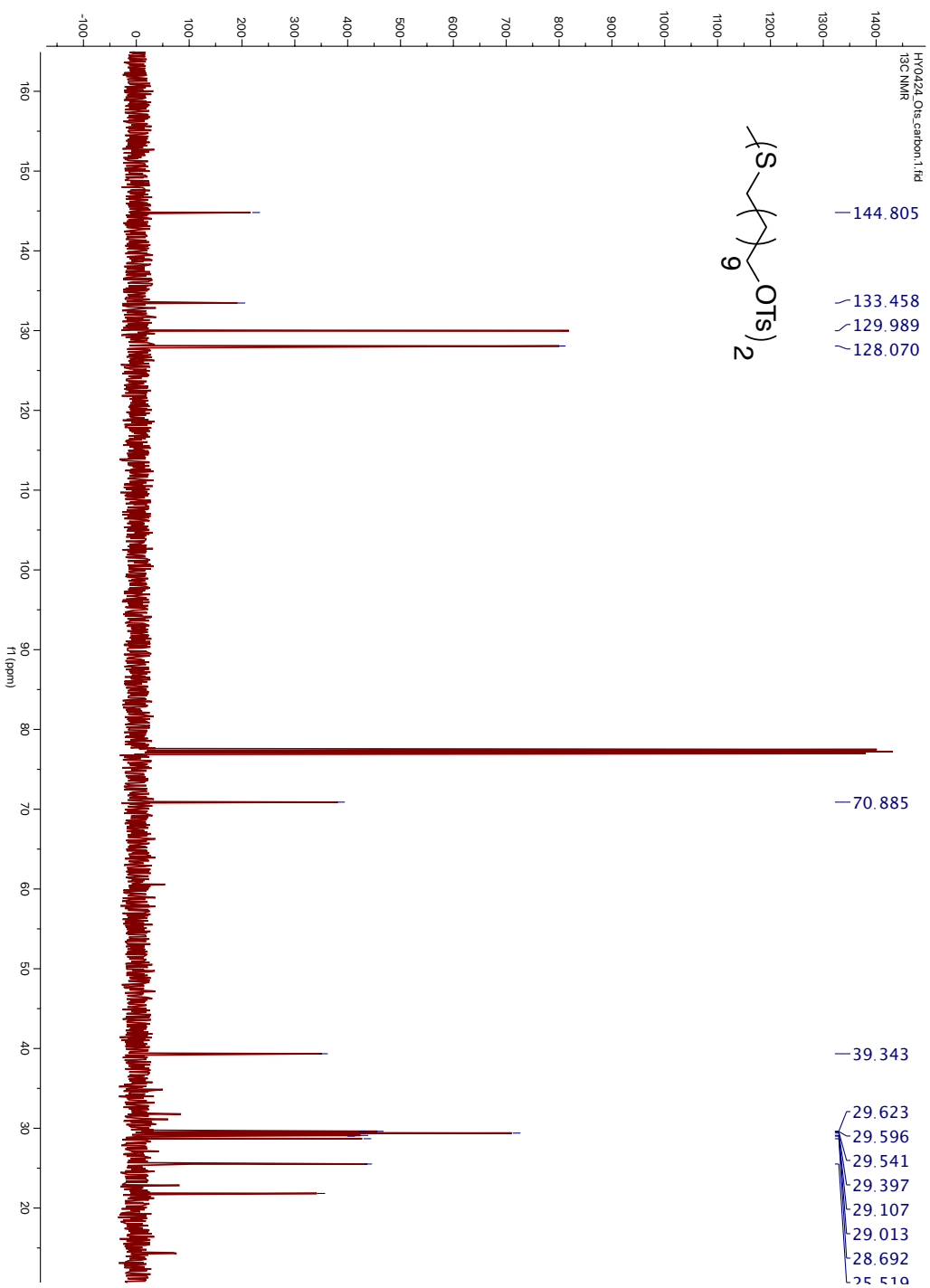

Appendix **2**. ^{13}C NMR of **6** in $CDCl_3$

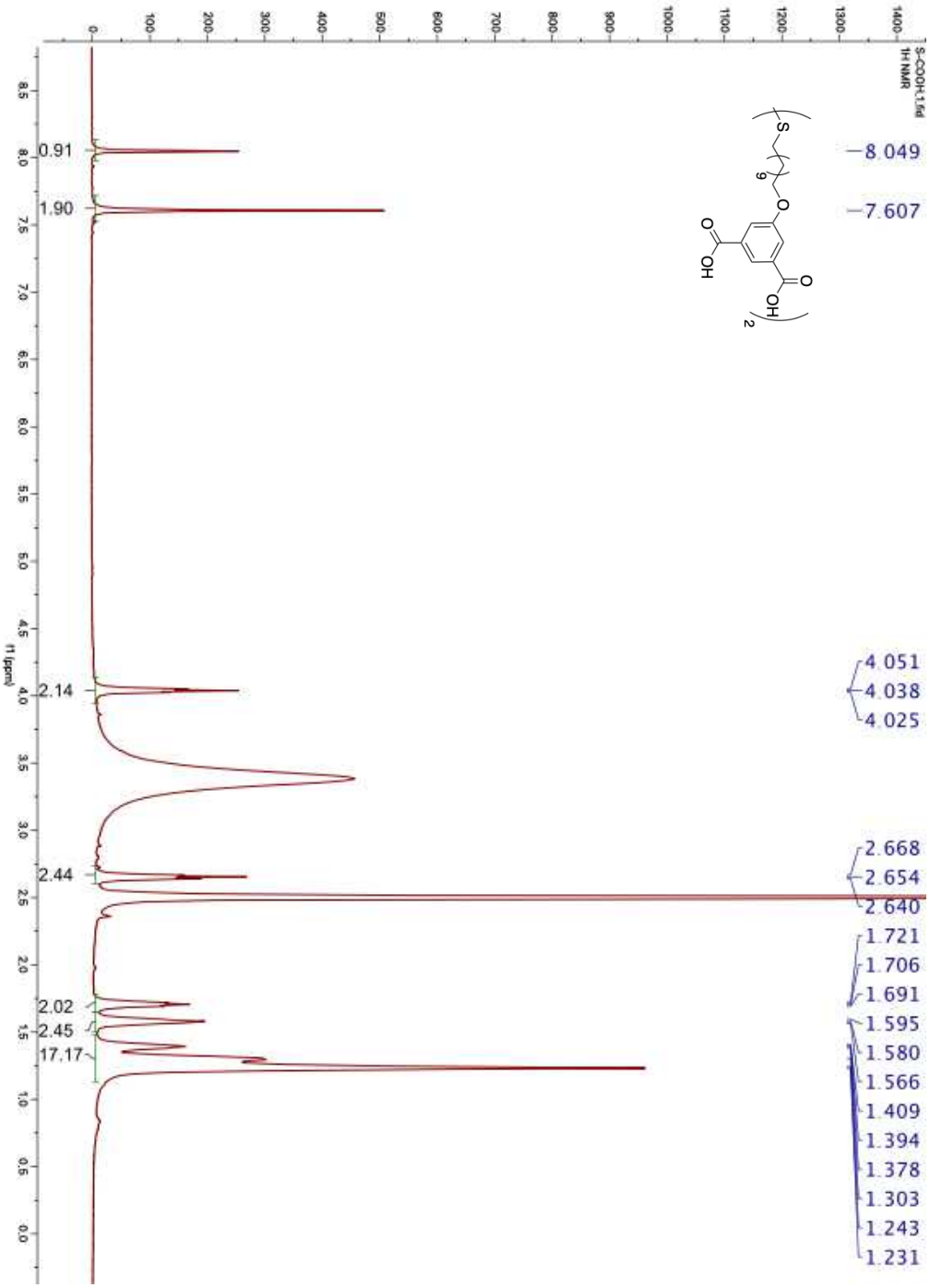

Appendix **3**. ^{1}H NMR of **1** in DMSO-*d6*

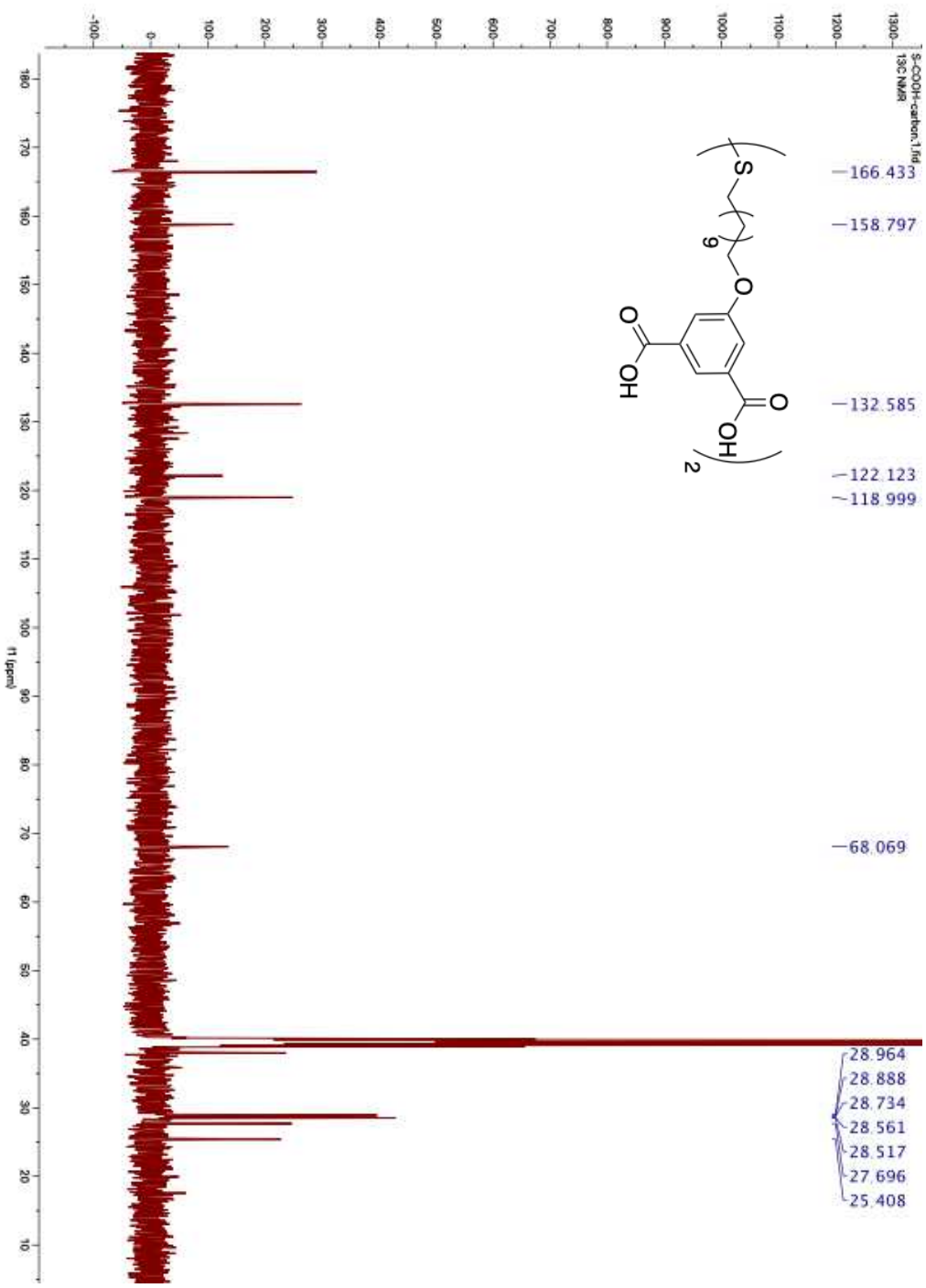

Appendix **4**. ^{13}C NMR of **1** in DMSO-d_6

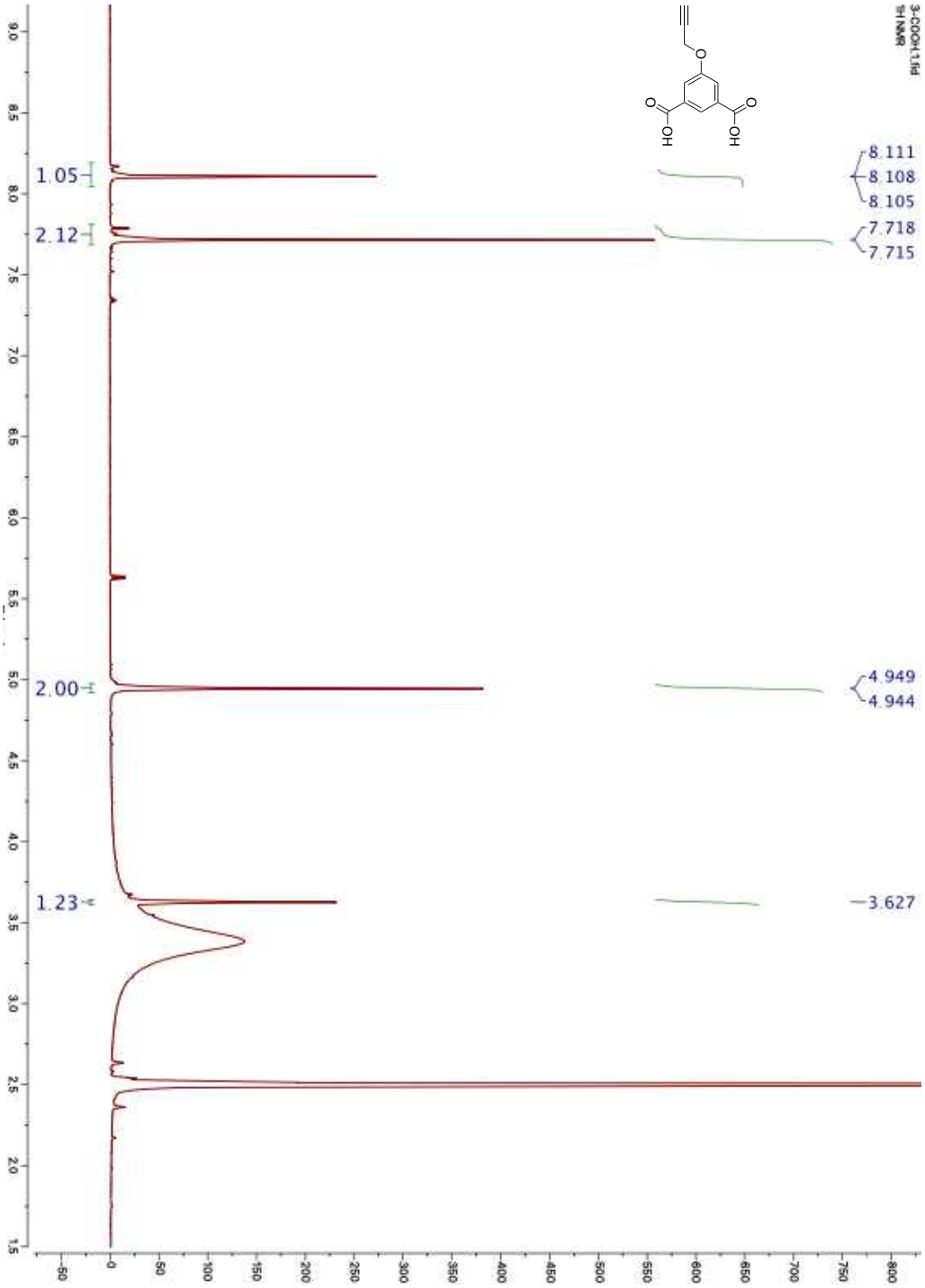

Appendix **5**. ^{1}H NMR of **2** in DMSO-d_6

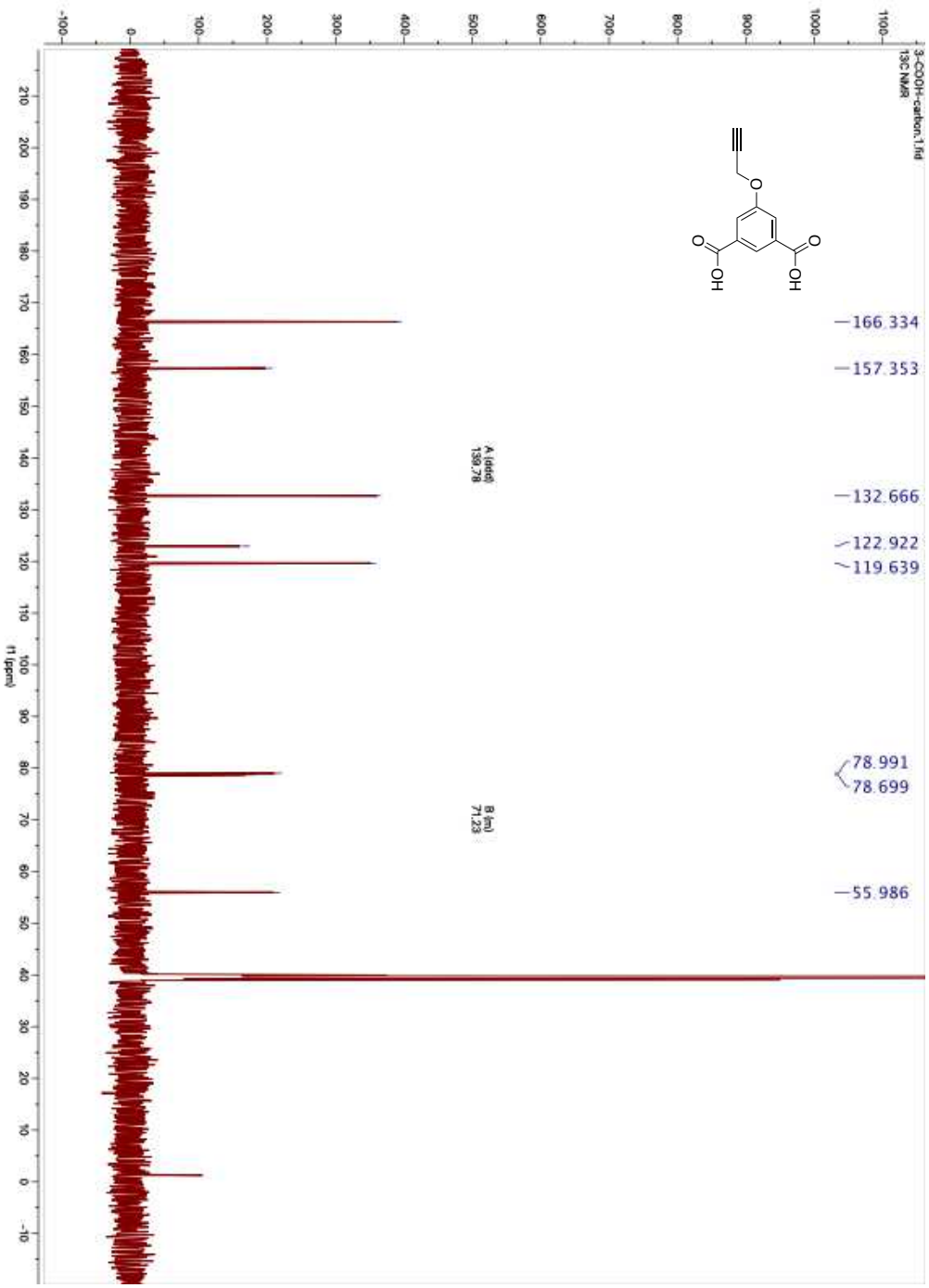

Appendix **6**. ^{13}C NMR of **2** in DMSO-d_6

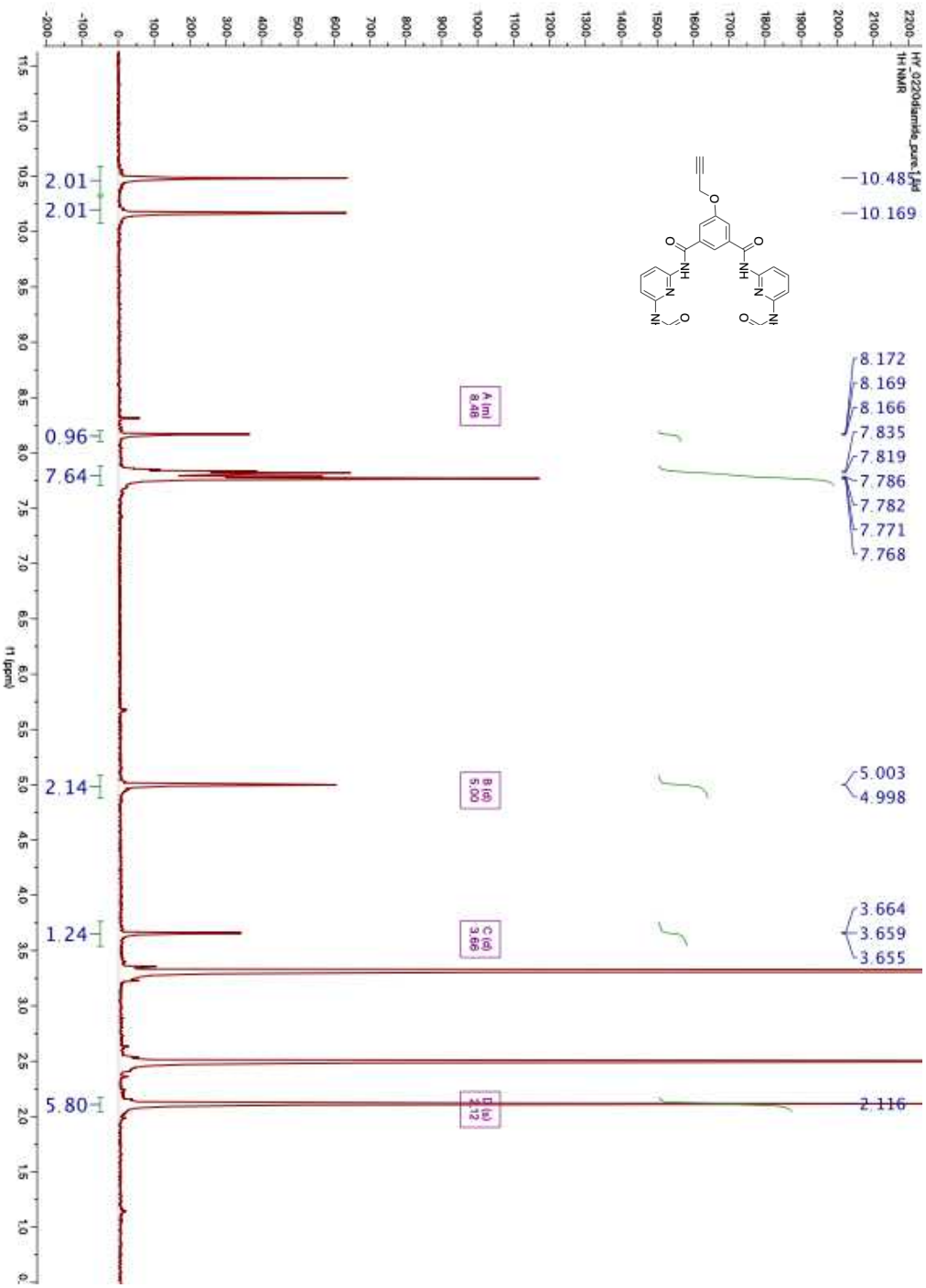

Appendix **7**. ^{1}H NMR of **9** in DMSO-d_6

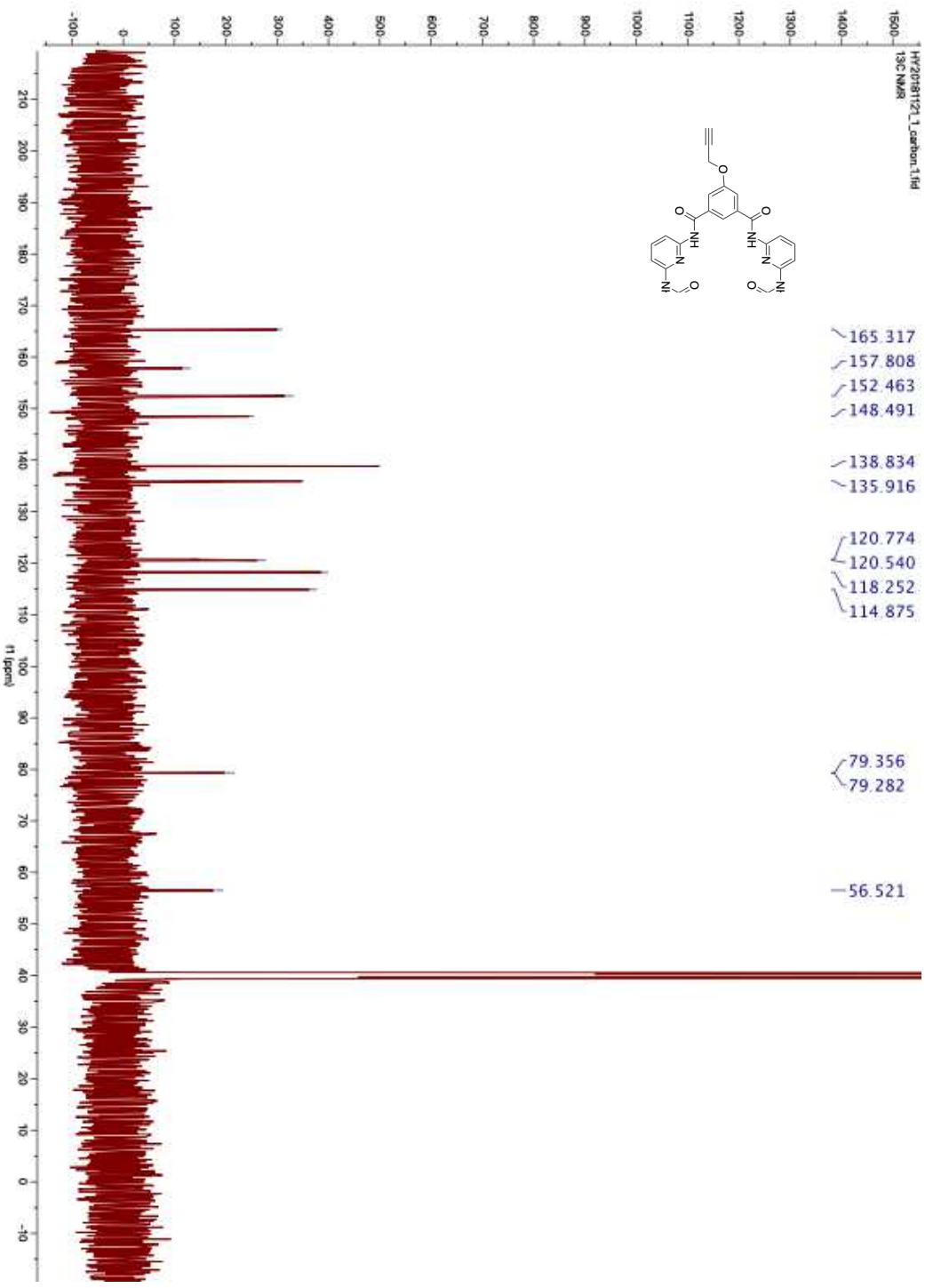

Appendix **8**. ^{1}H NMR of **9** in DMSO-d_6

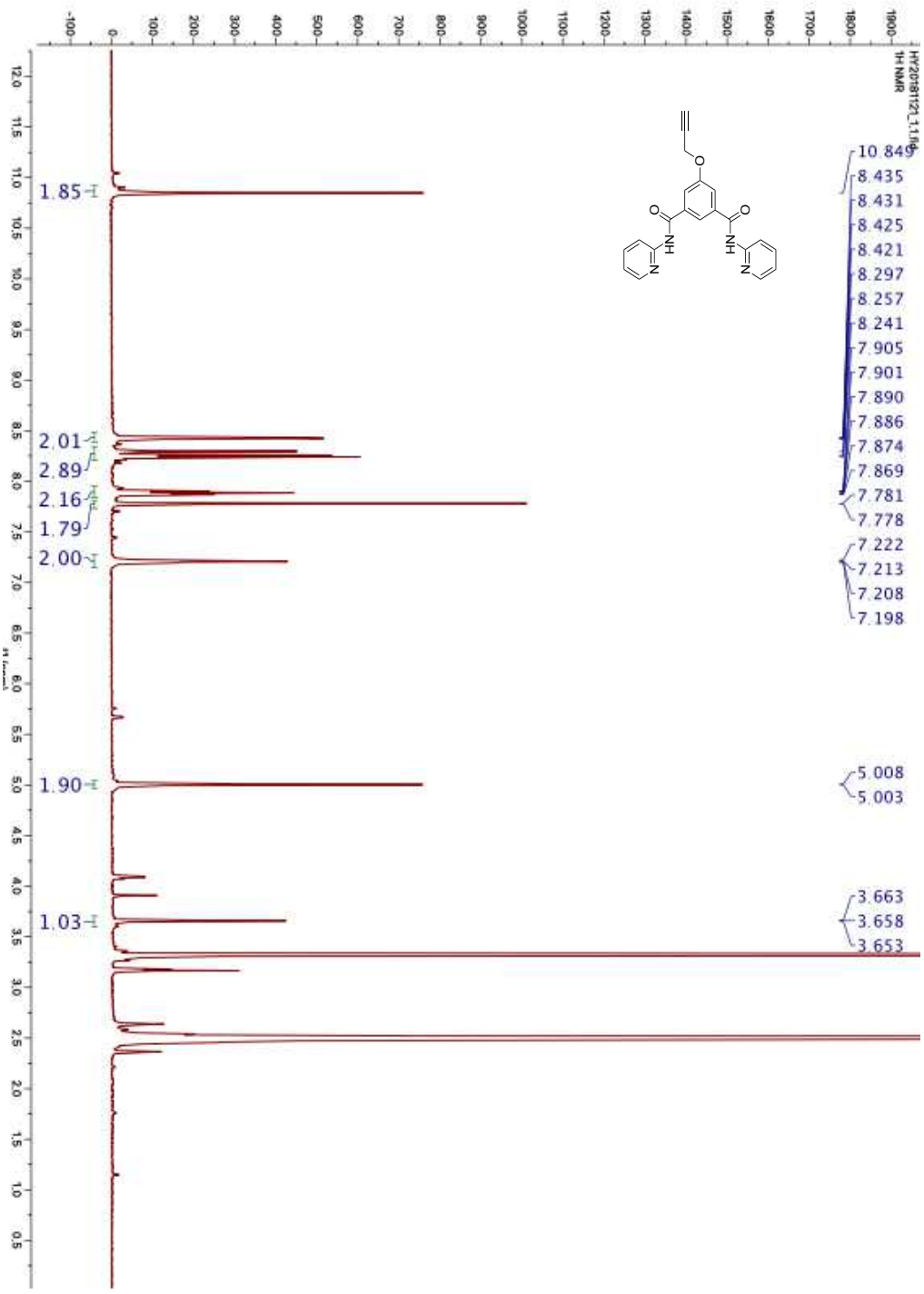

Appendix **9**. ^{1}HNMR of **11** in DMSO-*d*$_6$

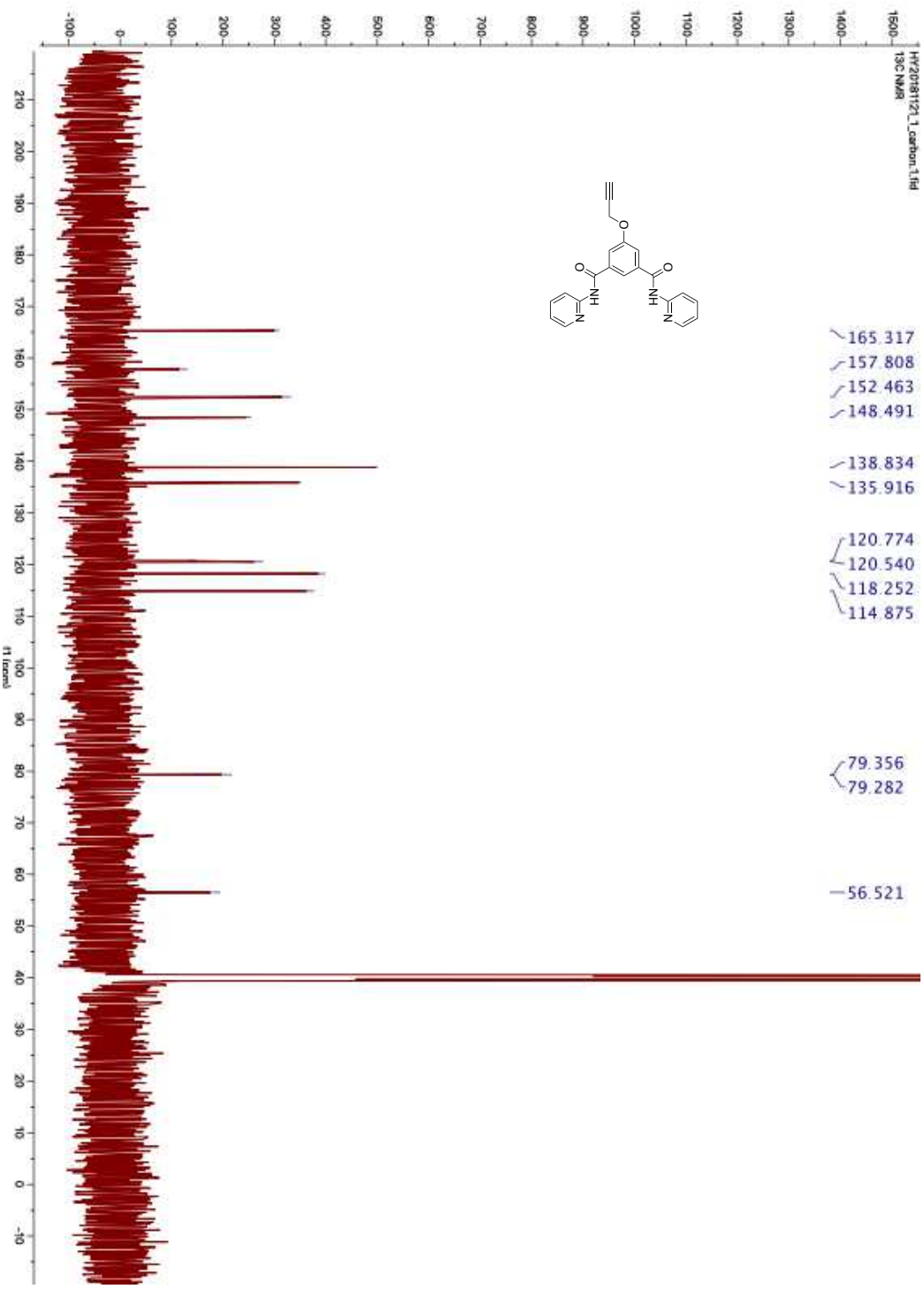

Appendix **10**. ^{13}C NMR of **11** in DMSO-d_6

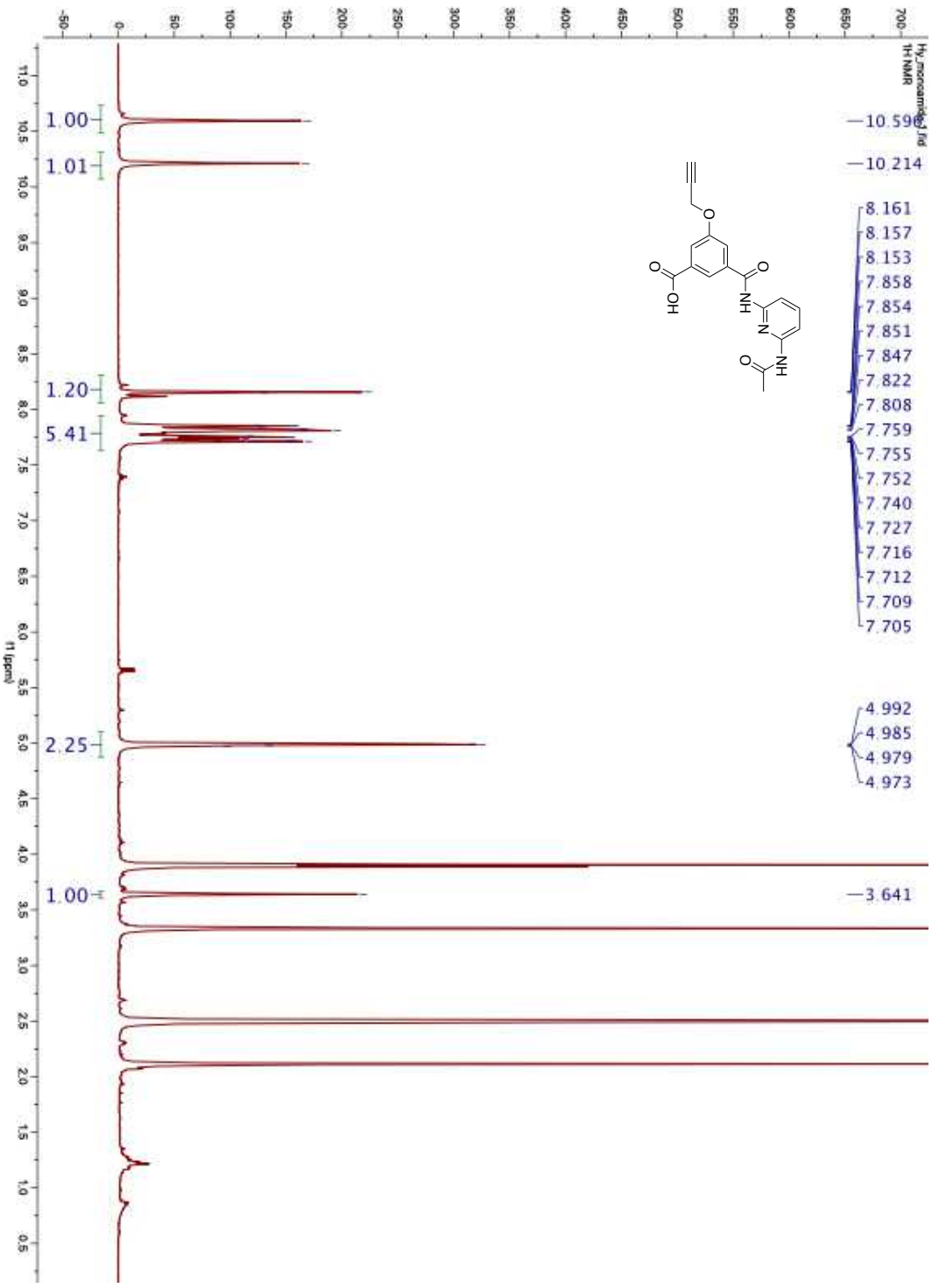

Appendix **11**. ^{1}HNMR of **10** in DMSO-*d*$_6$

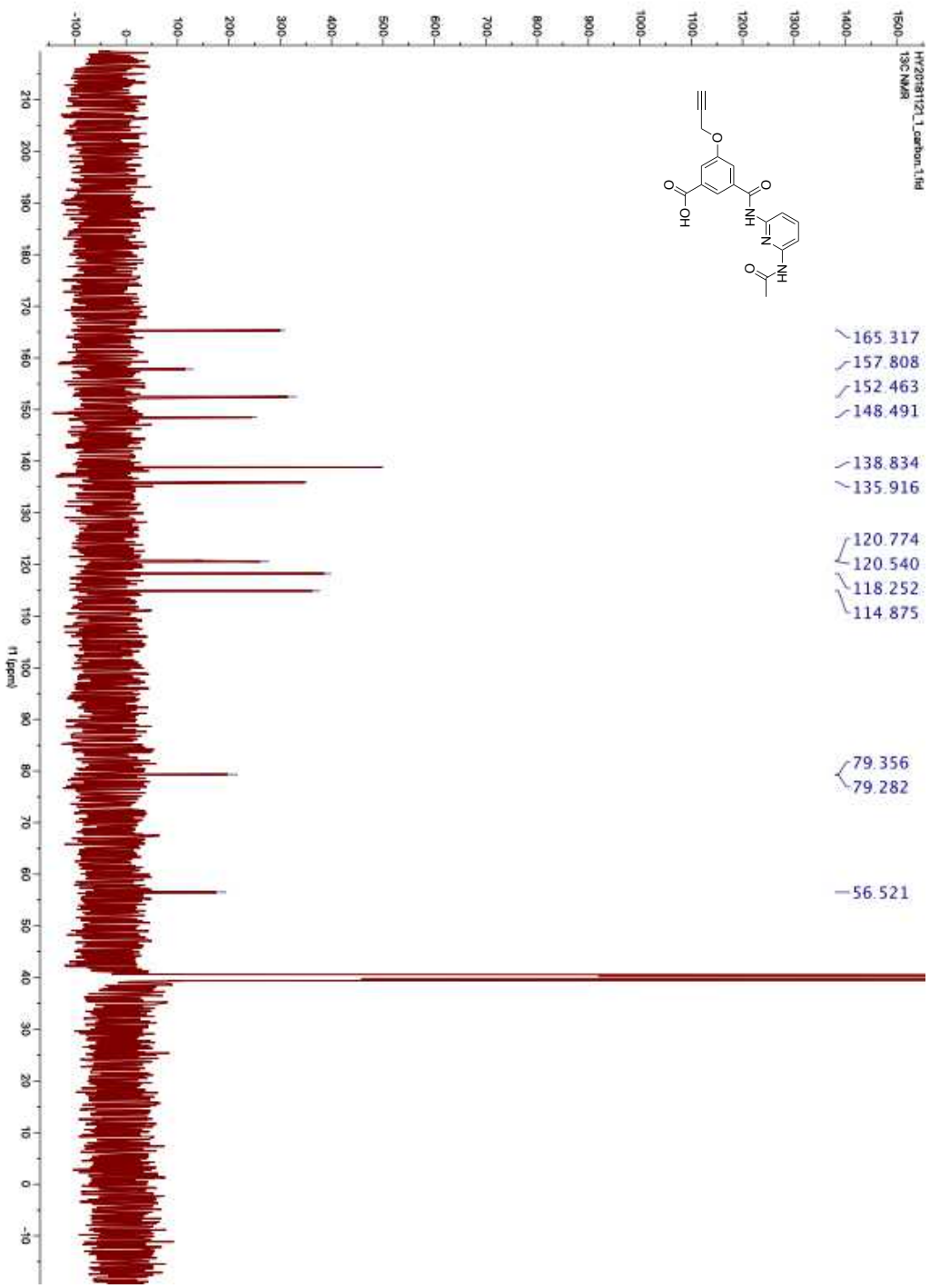

Appendix **12**. ^{13}CNMR of **10** in DMSO-d_6

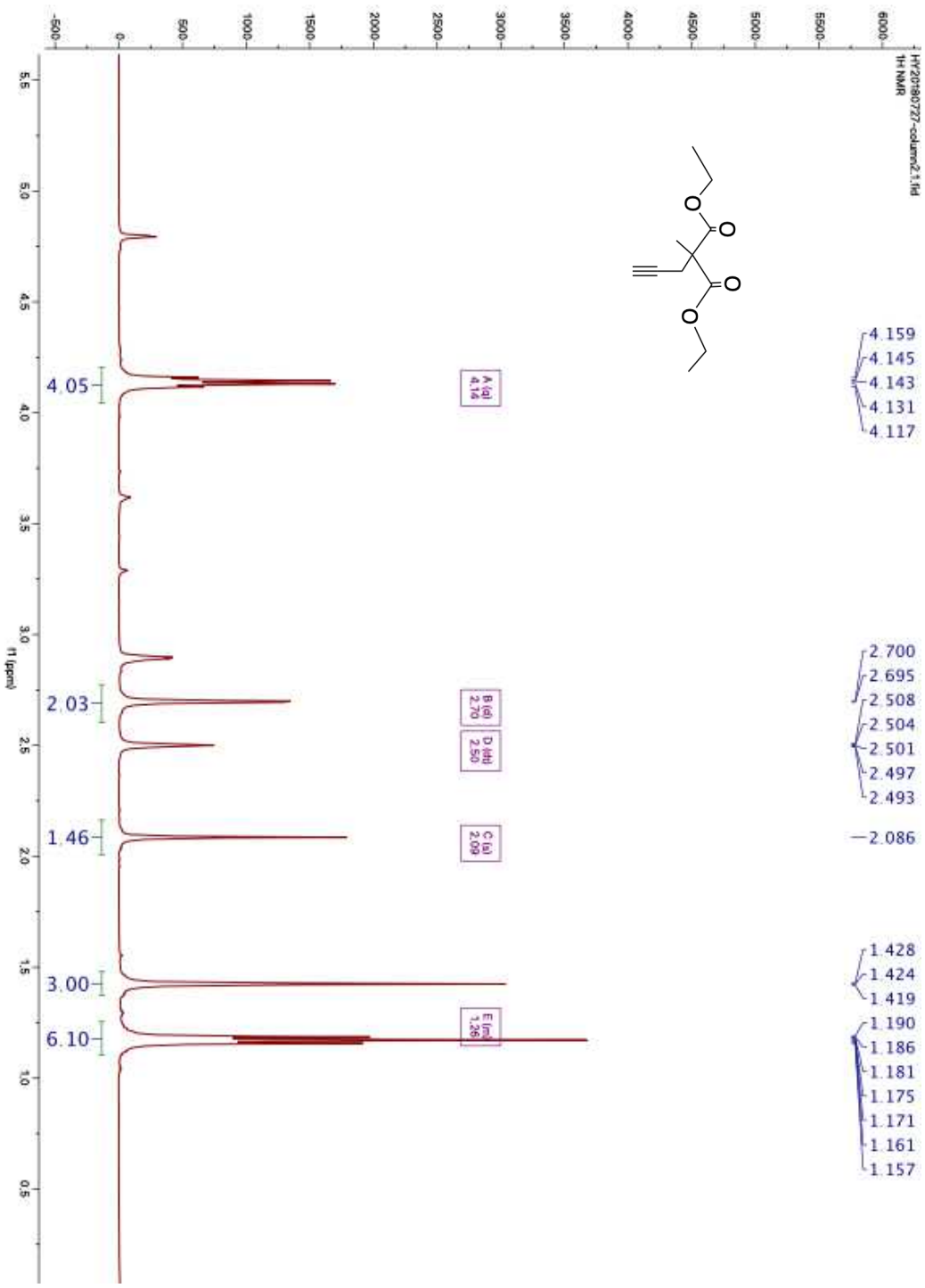

Appendix **13**. ^{1}H NMR of **12** in DMSO-*d*$_6$

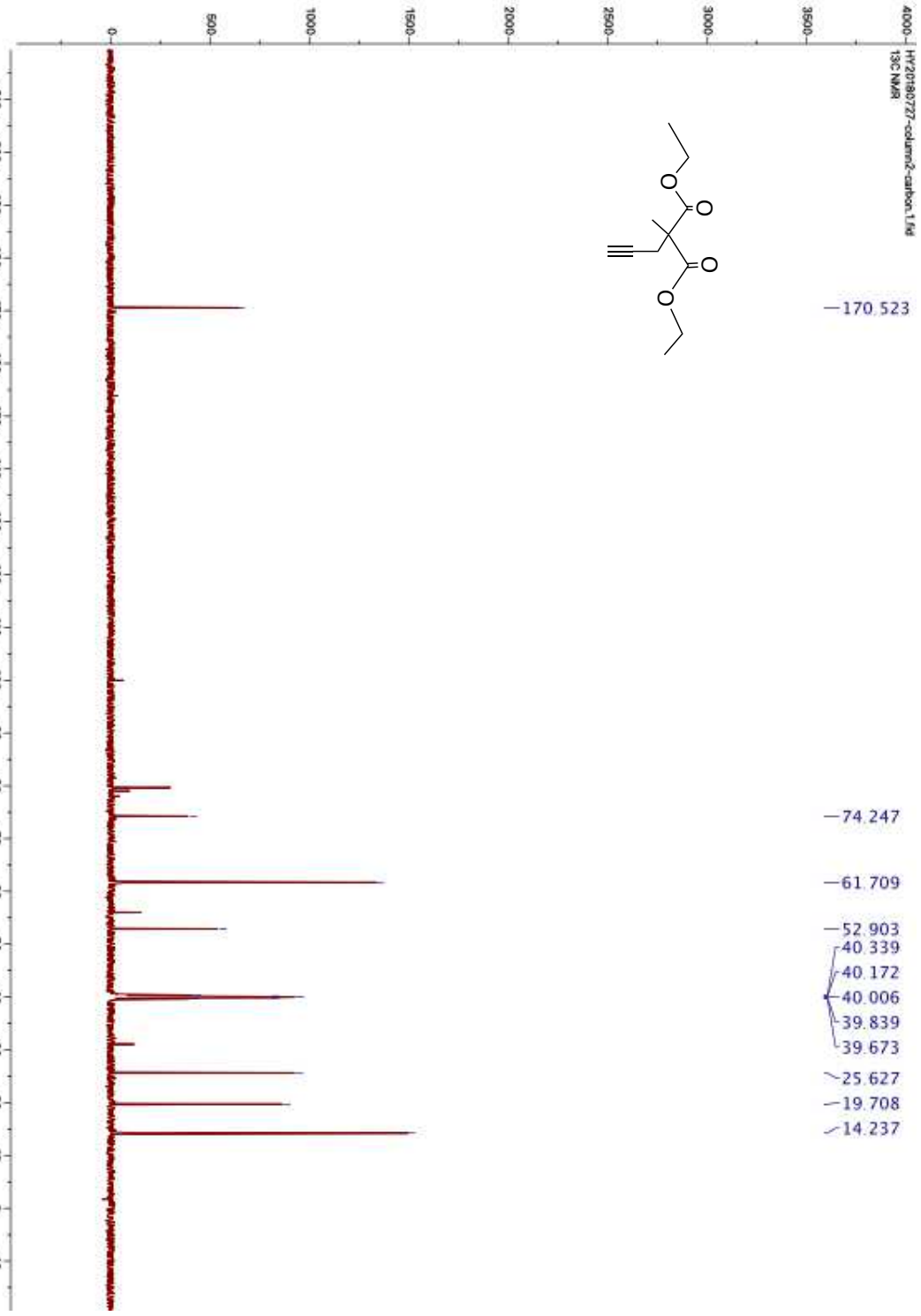

Appendix **14**. ^{13}C NMR of **12** in DMSO-d_6